Cours
Microplasmas: physique et applications

Claudia Lazzaroni

Laboratoire des Sciences des Procédés et des Matériaux,

Université Paris 13, Villetaneuse, France

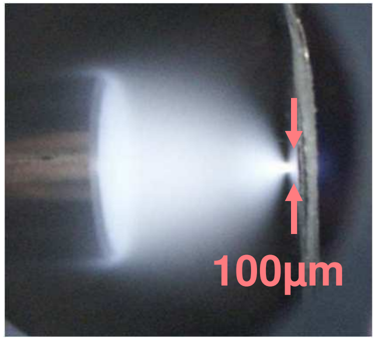

Journées Réseau Plasmas Froids 2018 – La Rochelle

Outline of the lecture

- Microplasmas: definition, interest and drawback

- Microplasma configurations

- Experimental characterization

Parameters of interest: T_g, n_e, *EEDF, reactive species density*

- Microplasma modeling

PIC simulation, fluid model, global model

- Applications of microplasmas: material synthesis and environment

Microplasmas: definition/applications

- Microplasma = plasma with submillimeter scale
- First works in the mid-90’s (Schoenbach *et al.*)
- High pressure stable glow discharge

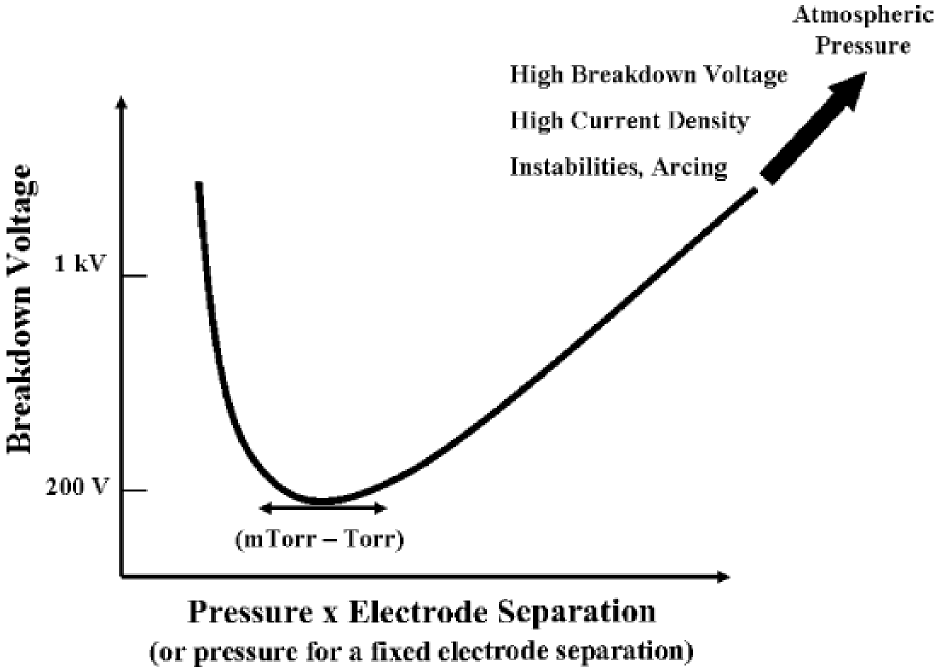

- Various applications: sterilization, treatment of human skin, light sources, micro-propulsion, synthesis of nanomaterials..

Interest and drawback of microplasmas

- Stable glow discharge at high pressure (intermediate to atmospheric pressure)

- Production of high density of reactive species → interesting for various applications such as lighting, material synthesis or medicine

But working surfaces and volumes are weak..

- Solution: microplasmas arranged in arrays or third electrode in the case of MHCD (→ MCSD)

Microplasma configurations (1)

- Micro Hollow Cathode Discharge (MHCD, 1996,USA):

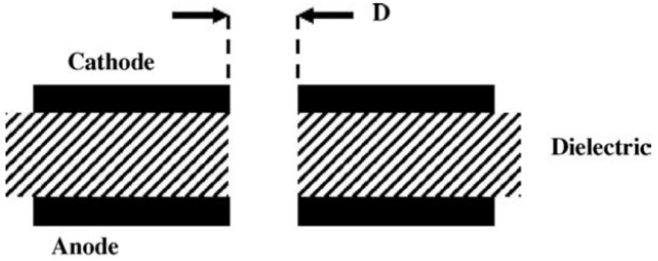

Schoenbach et al. APL ***68*** *(1996) 13*
Boeuf et al. APL ***86*** *(2005) 071501*
Aubert et al. PSST ***16*** *(2007) 23*

- Capillarity plasma electrode Discharge (CPED, 1997, USA):

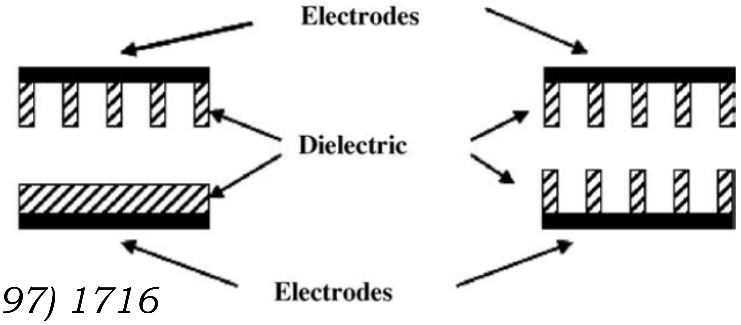

Kunhardt et al. BAMS ***42*** *(1997) 1716*

- D= 0,01-1 mm
- L/D = 10:1 – 1:1
- Pulsed DC or AC voltages

- Cathode Boundary Layer (CBL, USA):

Foest et al. PPCF ***47*** *(2005) B525*

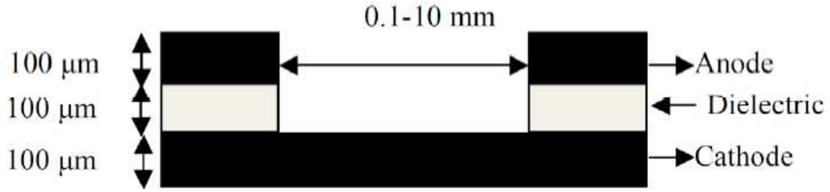

- Efficient source of excimer radiation
- Matrix easy to ignite

Microplasma configurations (2)

- Dielectric Barrier Discharge Microplasma (DBD,USA)

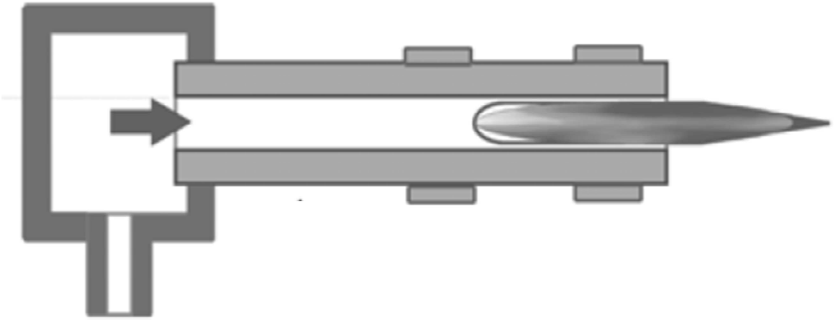

- RF excitation
- Surface modification

*Moselhy et al. JAP **95** (2004) 1642*

- Atmospheric pressure plasma jet (APPJ, Bochum/Belfast):

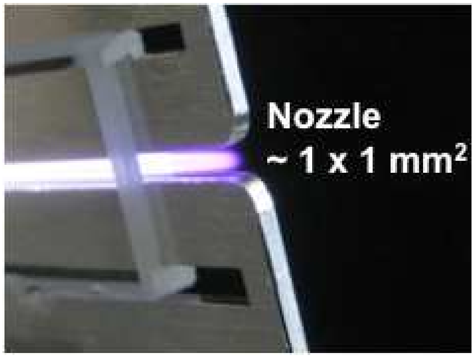

- RF excitation
- Electrode spacing : 1 mm

*V. Schulz-von der Gathen et al., J. Phys. D **41** (2008) 194004*

Increasing the plasma surface / volume

- Array of microplasmas:

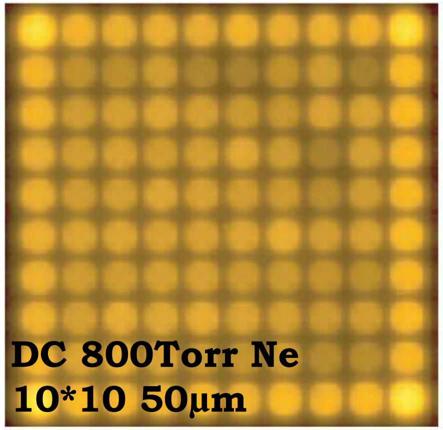

Eden et al. JPhysD ***38*** *(2005) 1644*

CBL
50mbar Ar
19*800µm

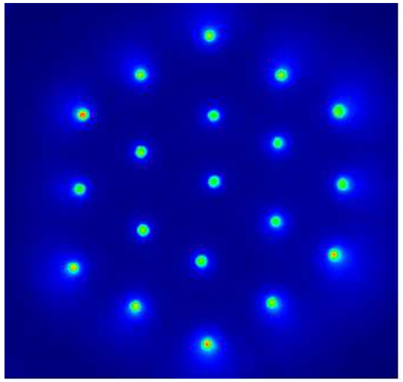

Martin et al. ICPIG 2012

Si/SiO$_2$/Ni MHCD
350mbar He
16*150µm

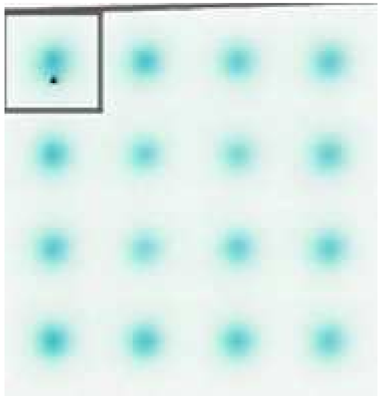

Felix et al. PSST ***25*** *(2016) 025021*

- MCSD

Ar
160 Torr

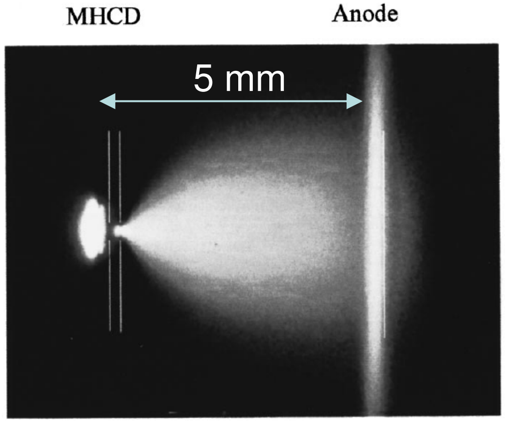

Eden et al. JAP ***85*** *(1999) 2075*
Makasheva et al. PPCF ***49*** *(2007) B233*

He/O$_2$/NO P$_{atm}$
O$_2$ ($^1\Delta$)

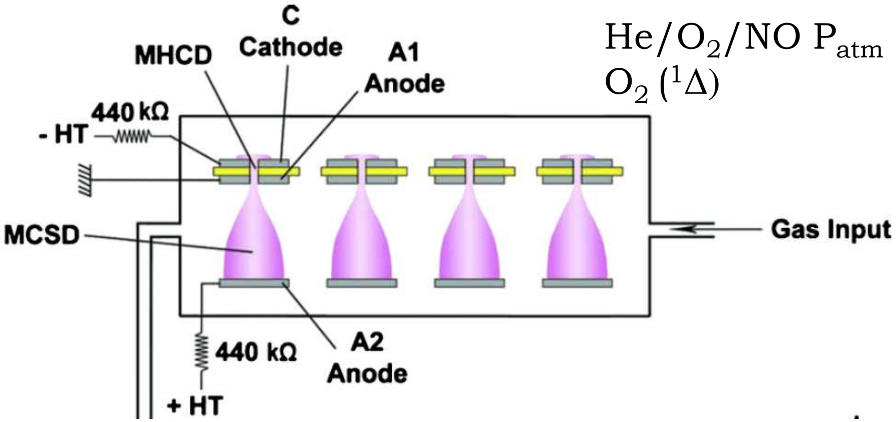

Santos Sousa et al. APL ***97*** *(2010) 141502*

Experimental characterization of microplasmas

- Diagnostics on microplasmas are challenging because of their small size

- Optical diagnostic methods: emission and absorption spectroscopy, interferometry, Thomson scattering

T_g measurement by OES

- Measurement of the spectrum of the first/second positive band of N_2 and comparison to a simulated spectrum (small admixture of N_2 needed if the gas mixture does not contain N_2)
- Example: Atmospheric-pressure air μdischarge

between two electrodes (2nd syst. positive)

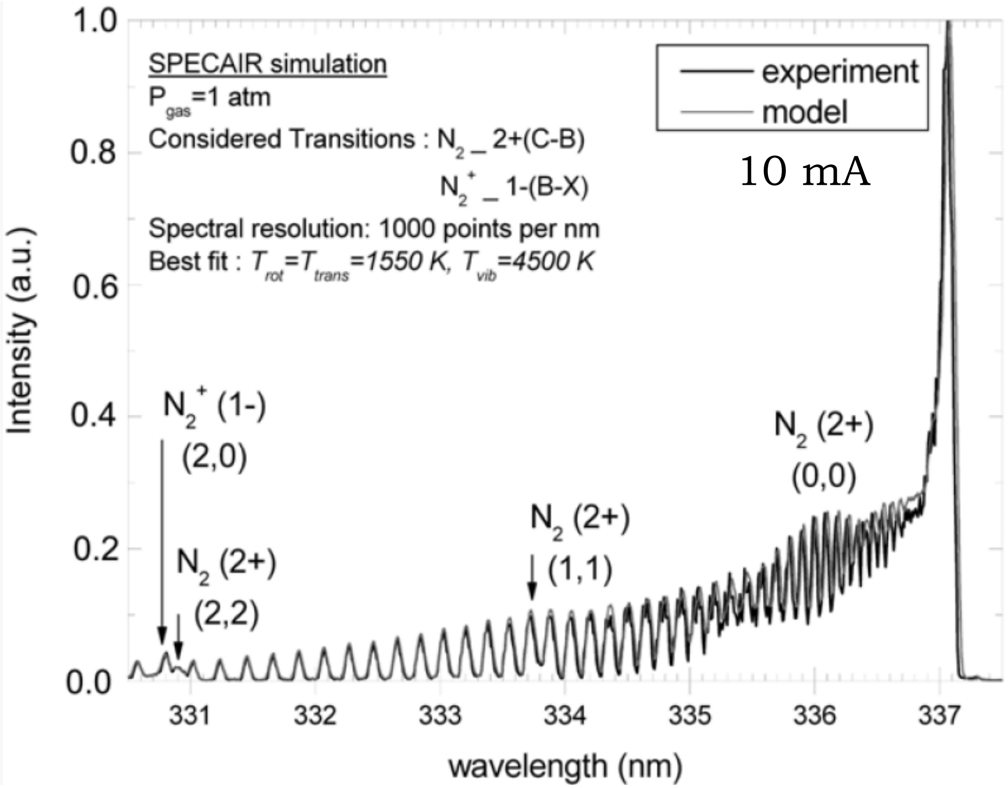

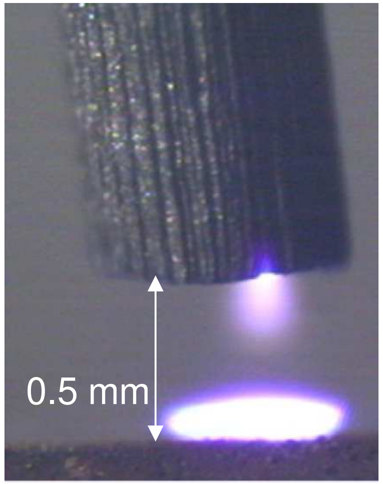

Staak et al. PSST ***14*** *(2005) 700*

For a current of 0.4 mA:
T_{rot} = 700 K and T_{vib} = 5000 K

T_g measurement by OES

- Temperature in microdischarges operating in noble gases and/or lower pressure is considerably lower
- Example: MHCD discharge in Ar at 1 mA and 100 Torr (1st system positive $B^3\Pi_g \rightarrow A^3\Sigma_u$)

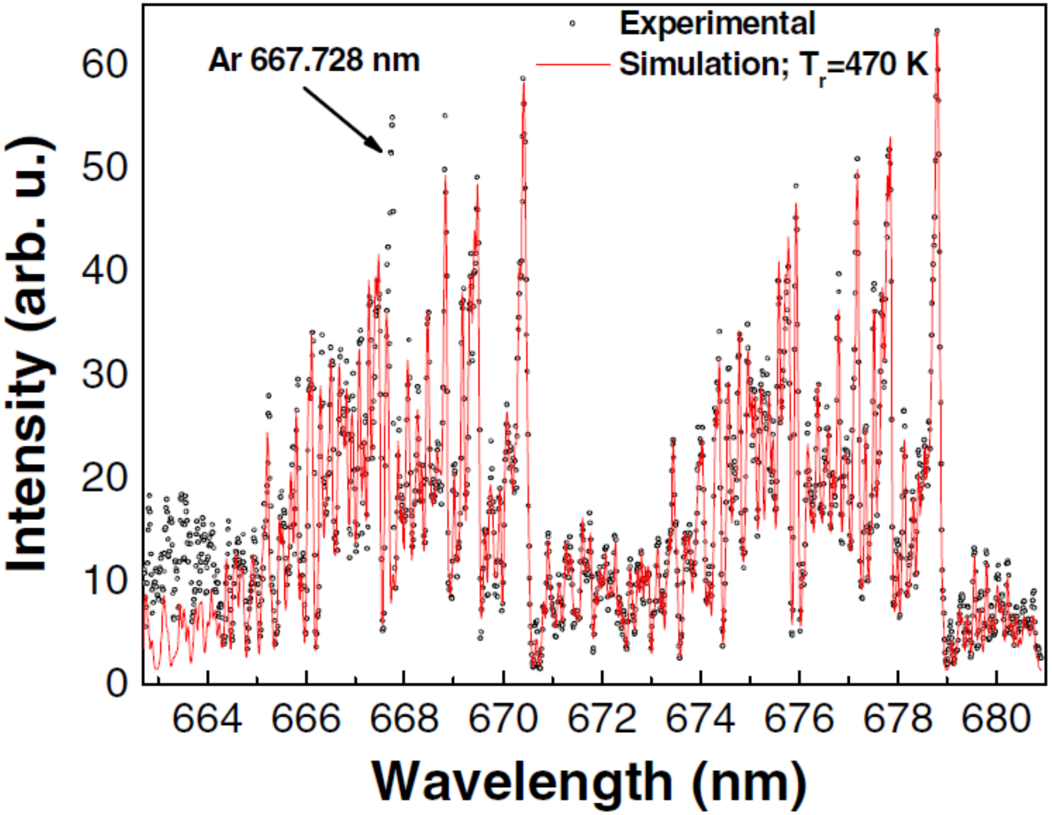

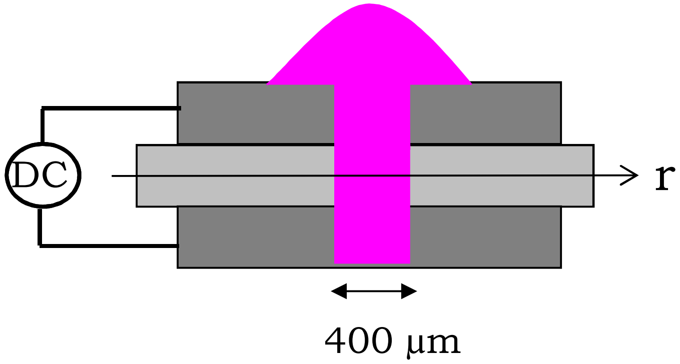

Lazzaroni et al. JPhysD ***43*** *(2010) 124008*

Radial dependence of T_g constant

Increase of T_g with the discharge current

T_g measurement by absorption spectroscopy

- High-pressure dc glow discharge based on micro-structured-electrode arrays in Ar at 0.5 mA (P = 50 to 400 mbar)
- Diode laser atomic absorption spectroscopy: Doppler broadening

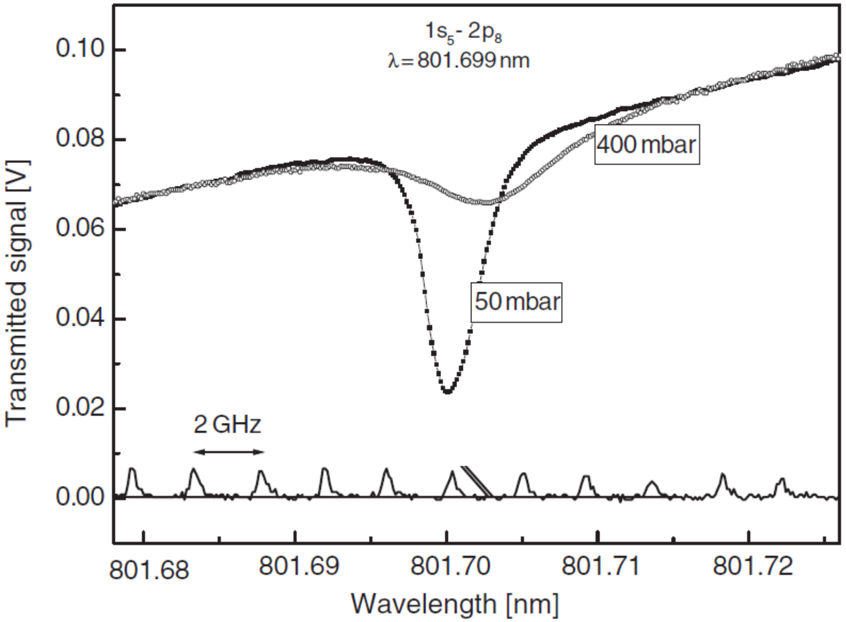

$$\Delta\lambda_G = 7.16 \times 10^{-7} \lambda_0 \sqrt{\frac{T}{M}}$$

Penache et al. PSST ***11*** *(2002) 476*

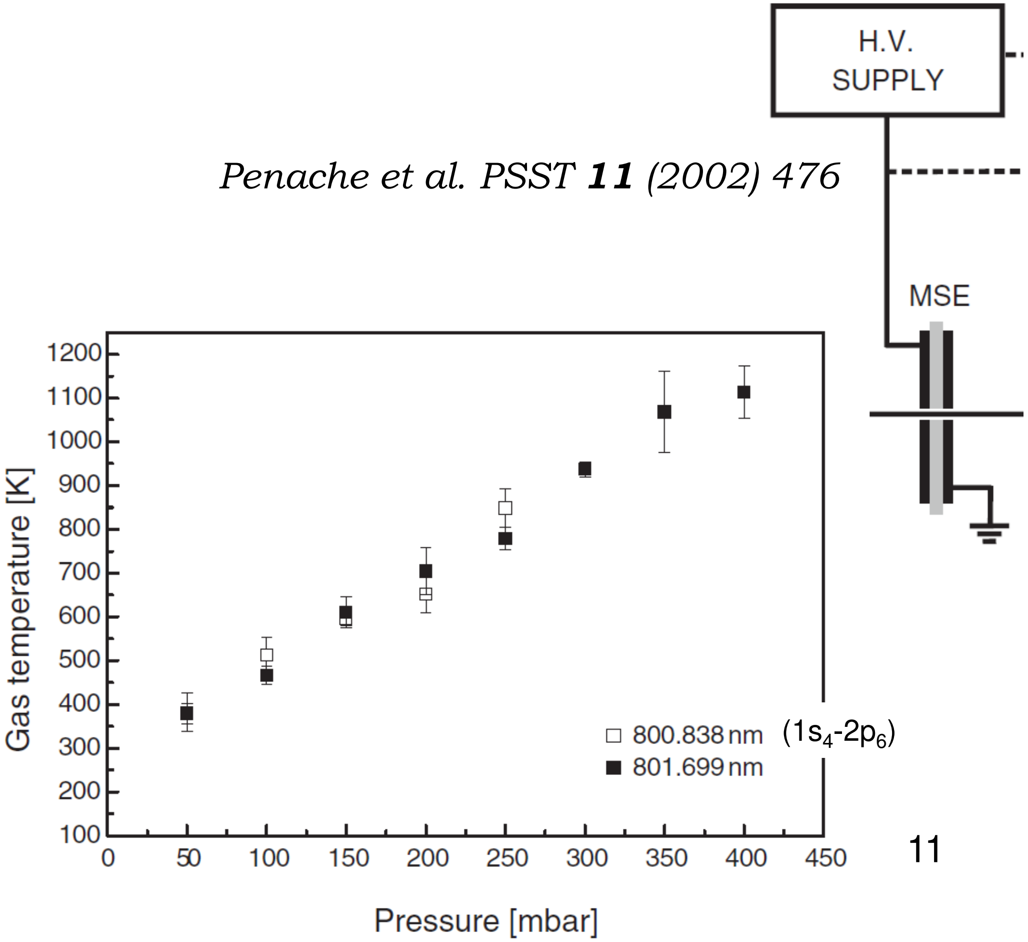

n_e measurement by OES

- DC MHCD at atmospheric pressure in Ar

Moselhy et al. JPhysD 36 (2003) 2922

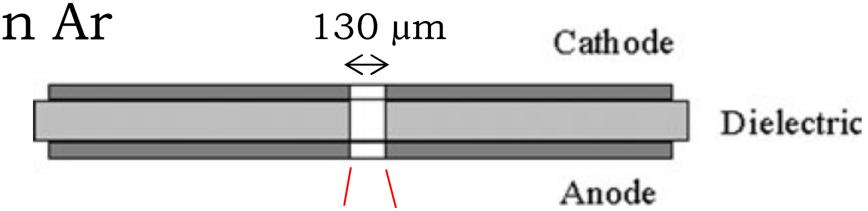

- Small admixture of H_2 to use the Stark broadening of the hydrogen Balmer-β line at 486.1 nm

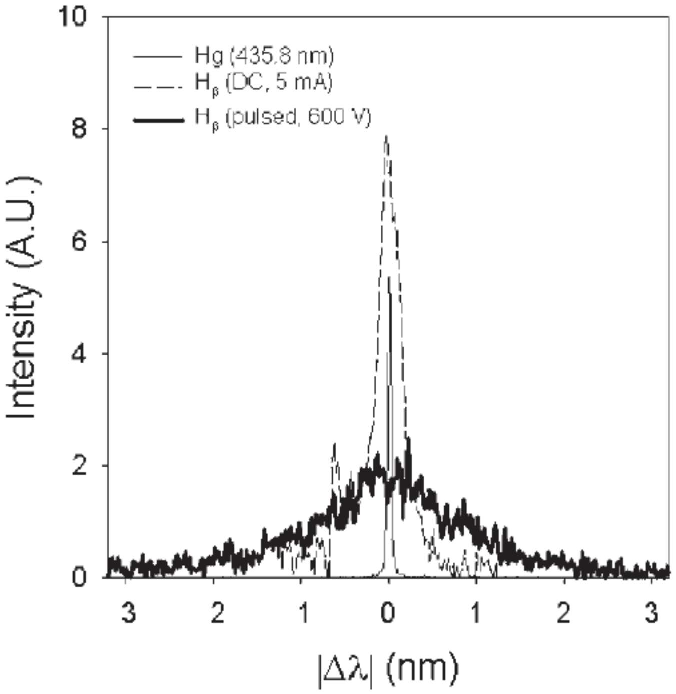

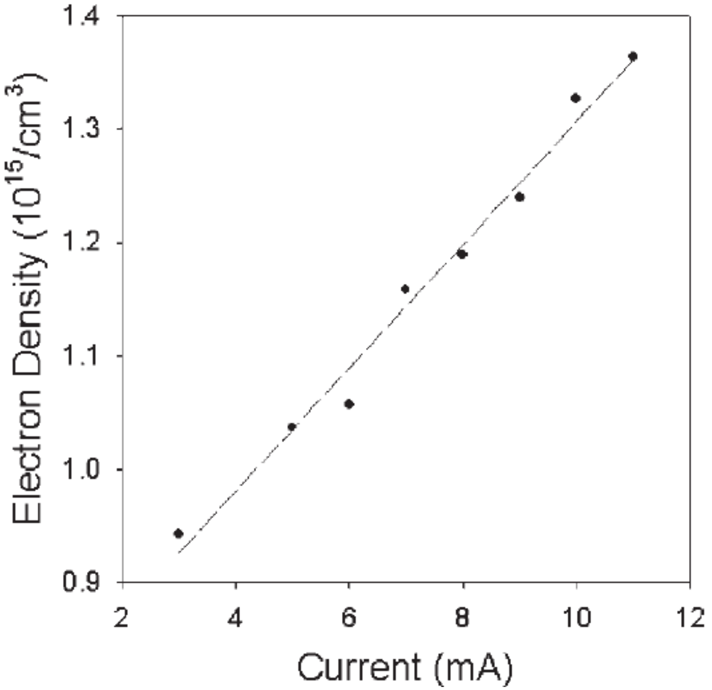

n_e in the pulse mode (600V, 10 ns, 10 mA) = 5.10^{16} cm^{-3}

n_e measurement by OES

- 3 nanosecond (2.46 kV, 10 kHz) pulsed atmospheric pressure argon microdischarge. Time-resolved OES
- Stark broadening of the 4p-4s Ar line at 696.54 nm

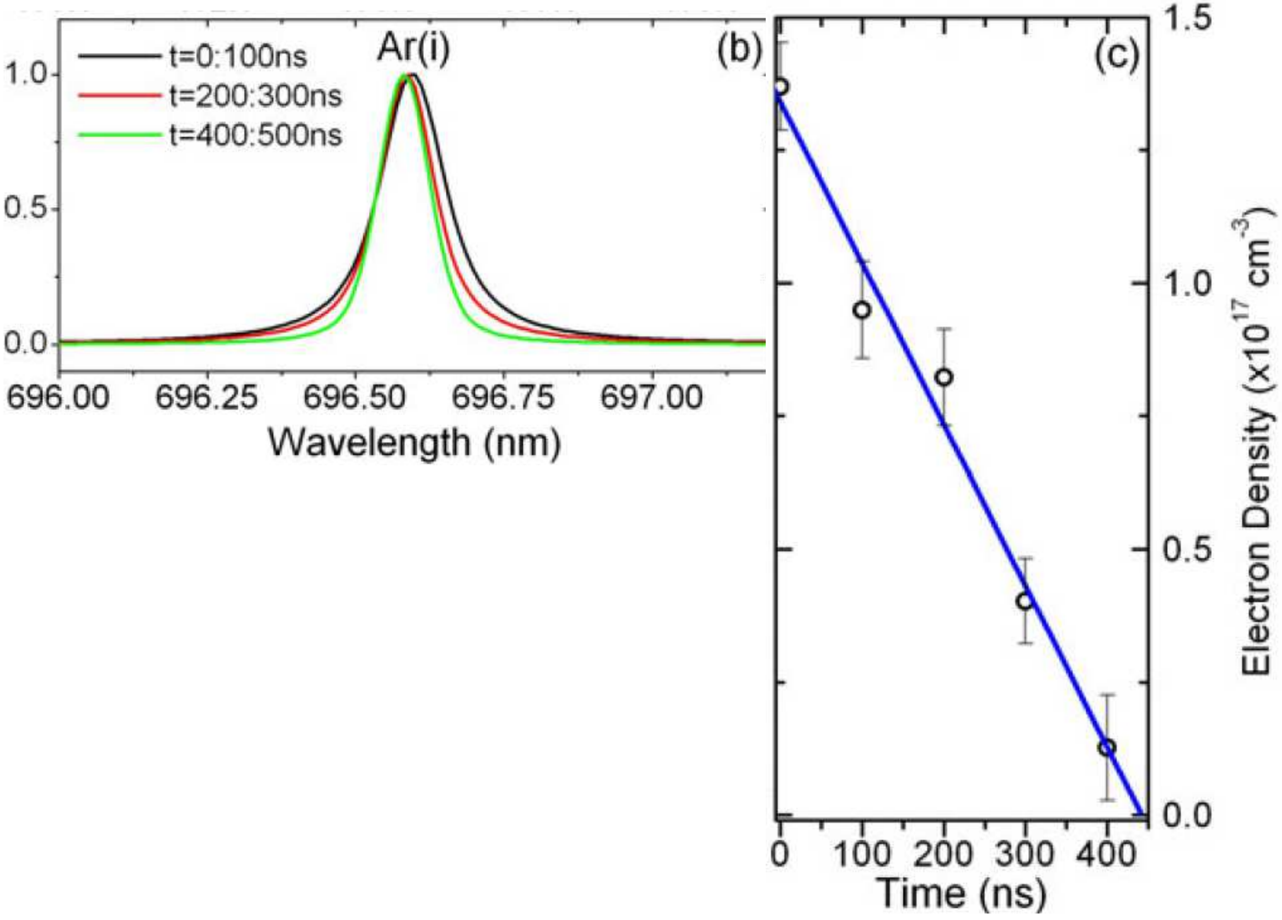

Walsh et al. EPJD ***60*** *(2010) 523*

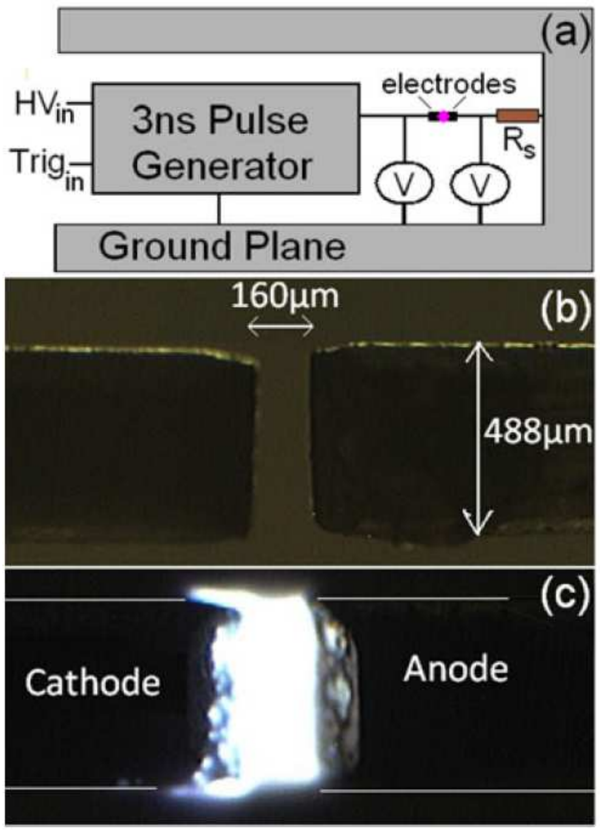

n_e measurement by Laser Thomson scattering

- Microdischarge between plane parallel electrodes (600 µm gap) in argon at intermediate pressure (300-700 Torr) for a current of 50 mA
- Use of the beam of a pulsed frequency-doubled Nd:YLF laser (λ = 526.5 nm, f = 3 kHz, τ = 100 ns, P = 6W)

Example of net Thomson spectrum

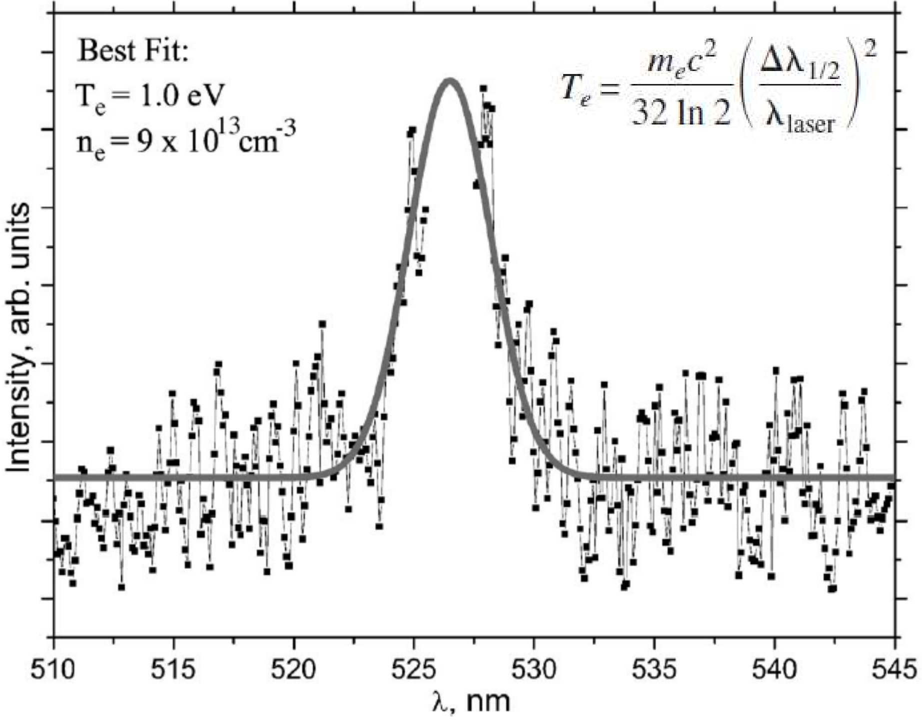

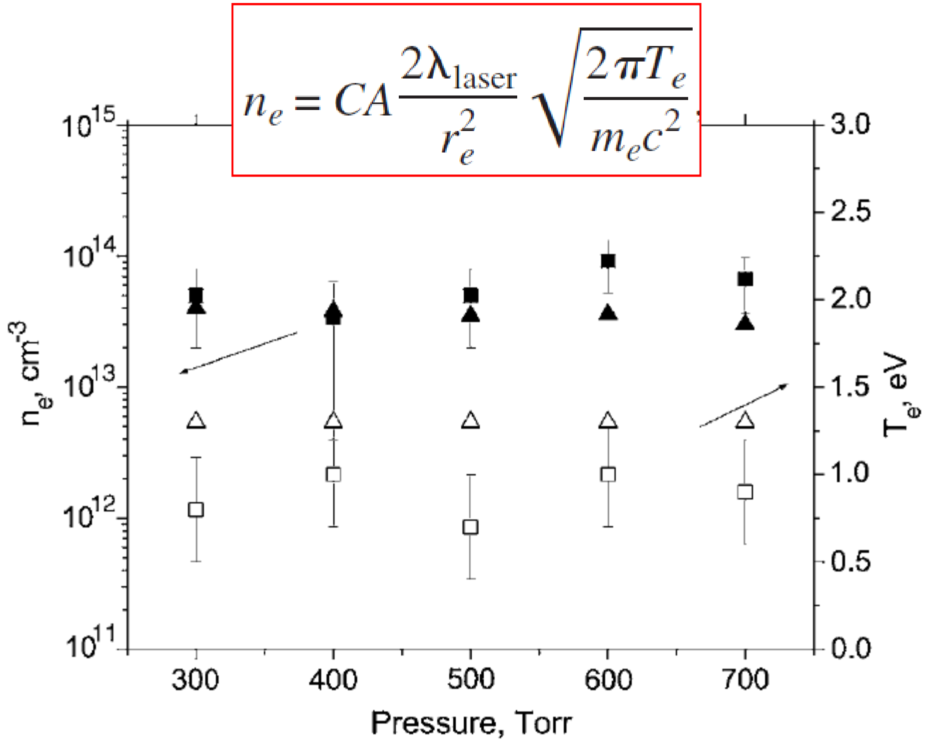

$$n_e = CA\frac{2\lambda_{laser}}{r_e^2}\sqrt{\frac{2\pi T_e}{m_e c^2}}$$

Belostotskiy et al. APL ***92*** *(2008) 221507*

Electron velocity distribution function

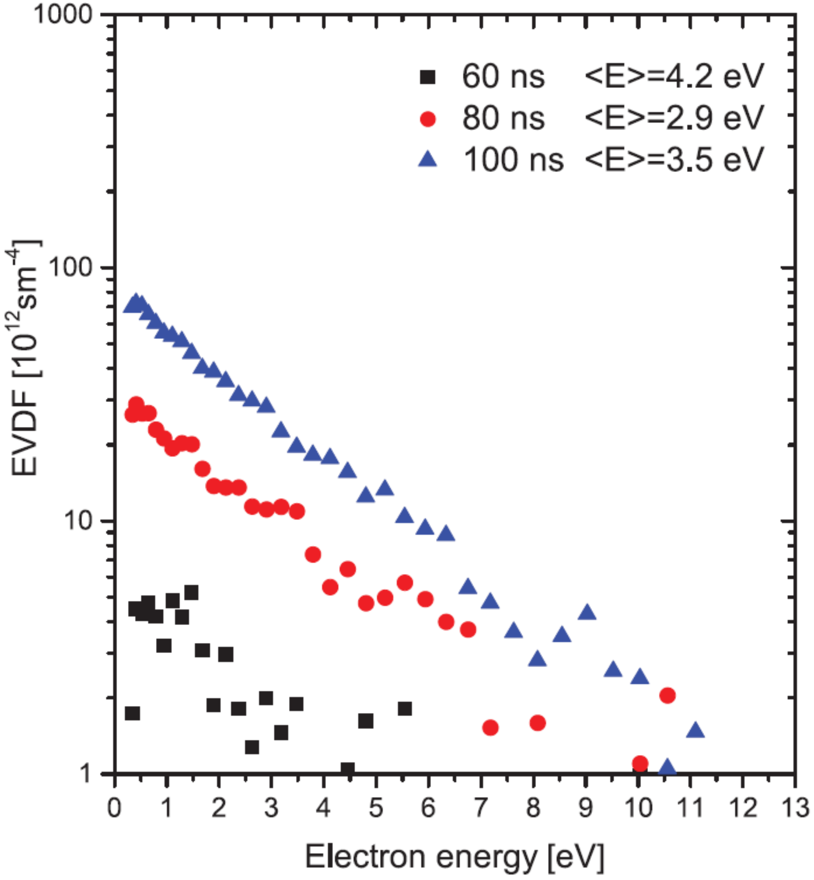

Schregel et al. PSST ***25*** *(2016) 054003*

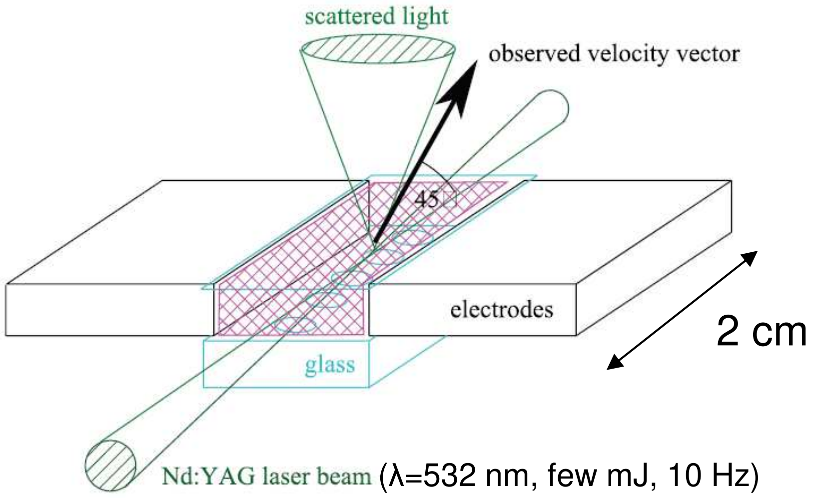

- 0.7 bar He microdischarge between planar electrodes (Mo) separated by a gap of 0.95 mm; 150 ns pulses with amplitude of 1 to 2 kV and f = 5 kHz
- Thomson scattering (elastic scattering on free electrons) → eedf in a range of energies up to 12 eV
- Maxwellian eedf <-> T_e = 3.5 eV at 100ns

Reactive species density: n_O

- Measurement of absolute atomic oxygen density by TALIF in a RF-APPJ in He/O_2

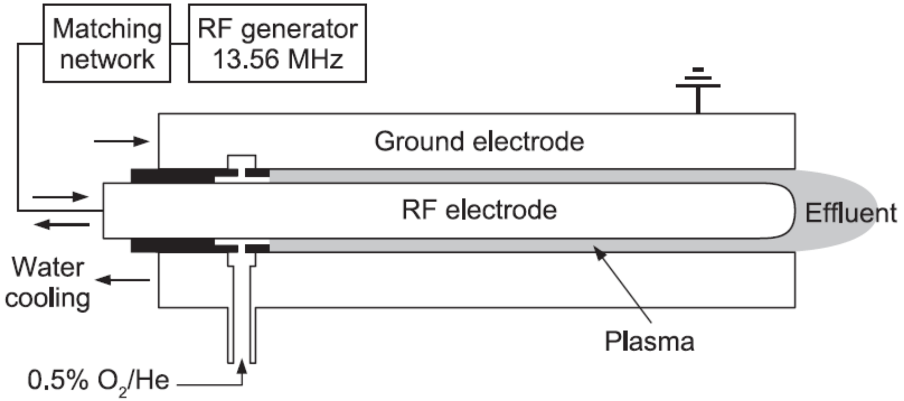

Niemi et al. PSST ***14*** *(2005) 375*

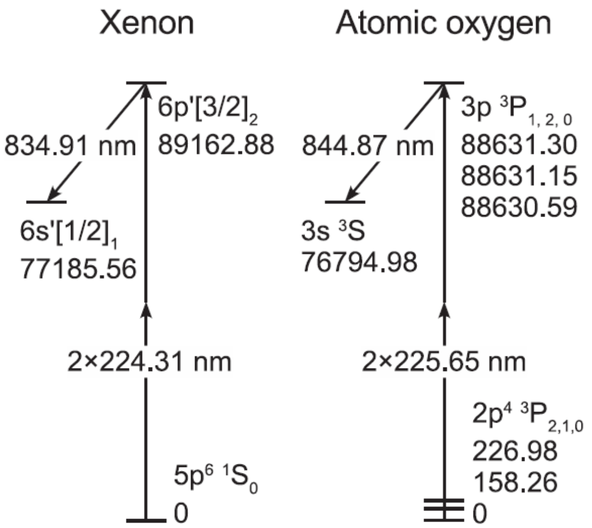

Two-photon excitation schemes

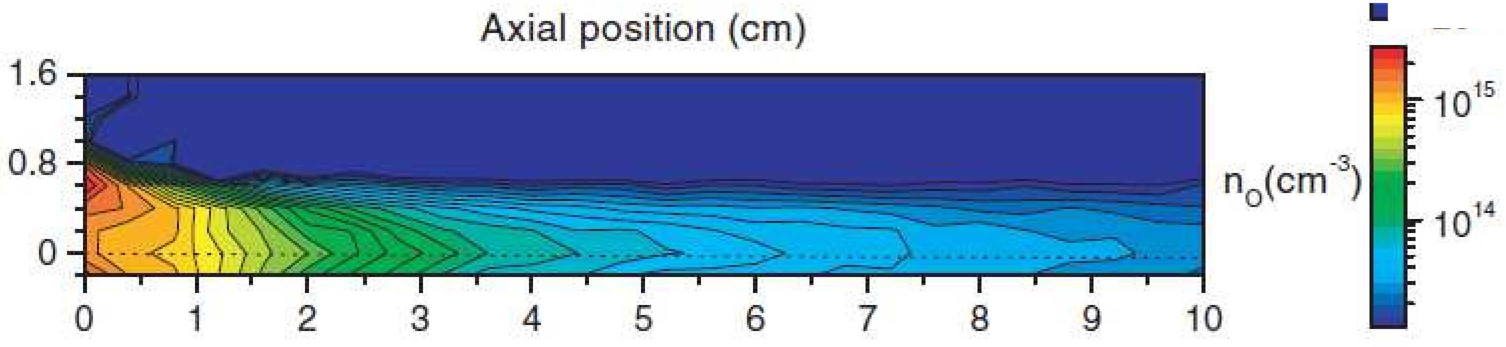

Reactive species density: n_{O2*}

Measurement of absolute O_2* density by infrared optical emission spectroscopy in a RF-APPJ in He/O_2: emission at 1.27 µm

*Sousa et al. JAP **109** (2011) 123302*

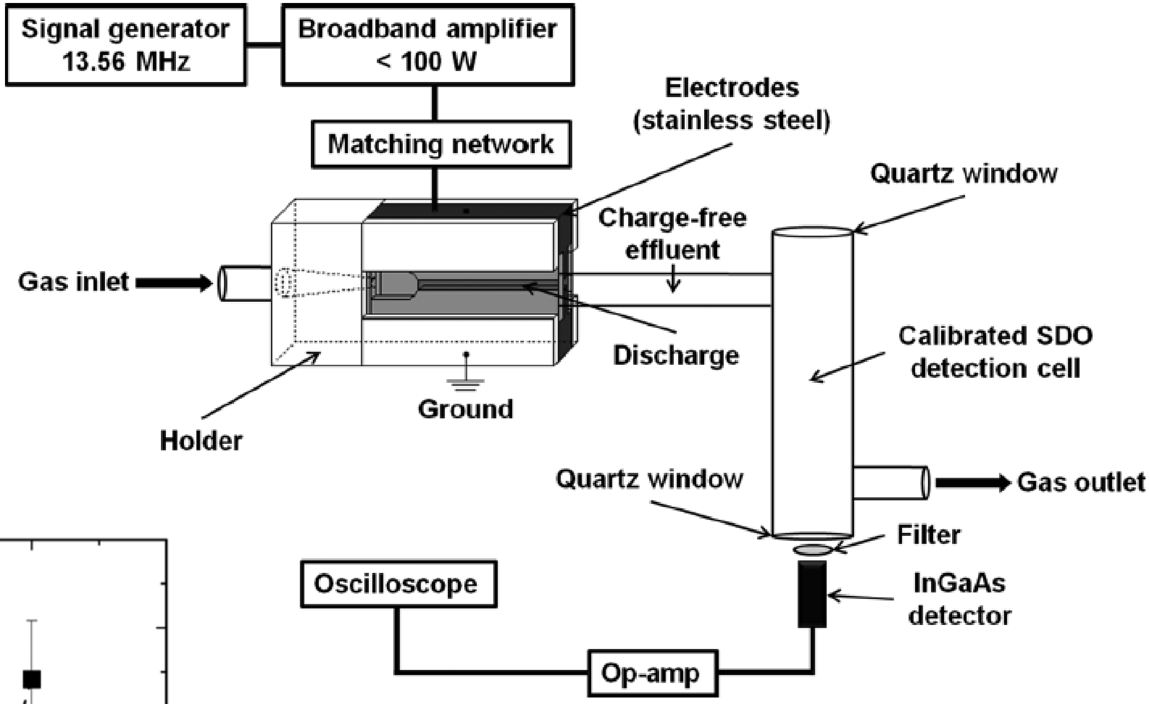

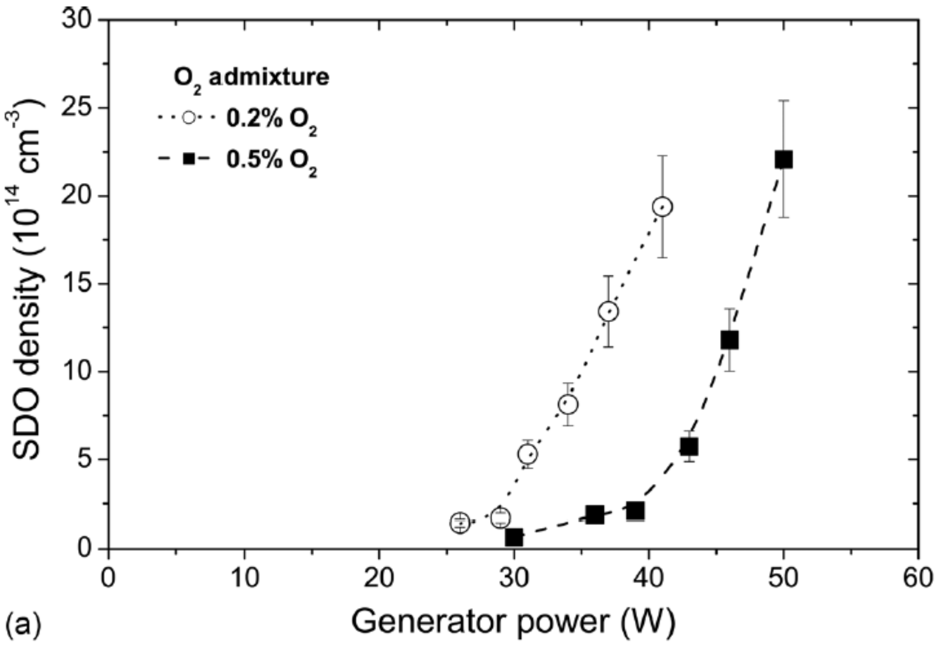

At larger O_2 admixture, shift towards higher power → energy consumption through molecular vibrational and rotational excitations, dissociations

Reactive species density: n_N

- Measurement of absolute atomic nitrogen density by VUV FTS
- Atmospheric pressure RF microplasmas in He/N_2/O_2 (d= 1mm)
- Transitions from the ground state to the quadruplet state located around 120 nm.

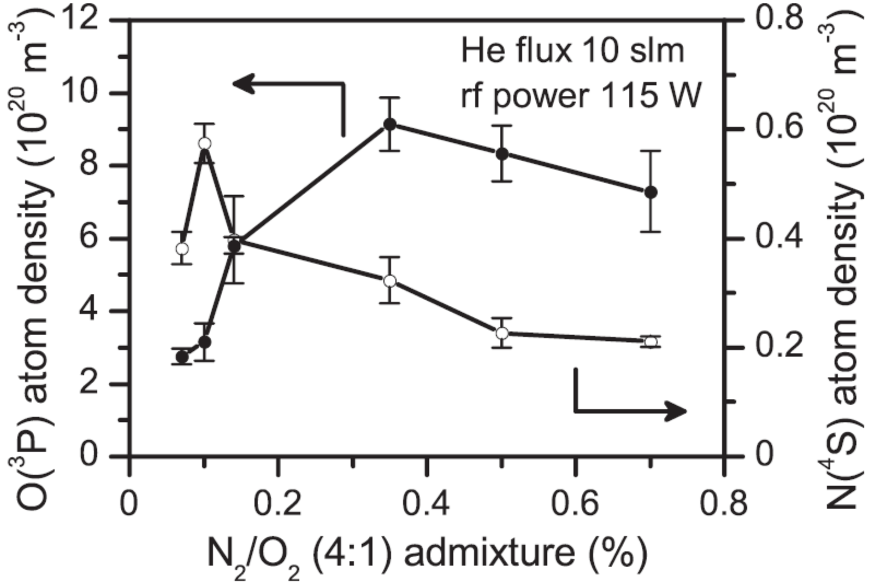

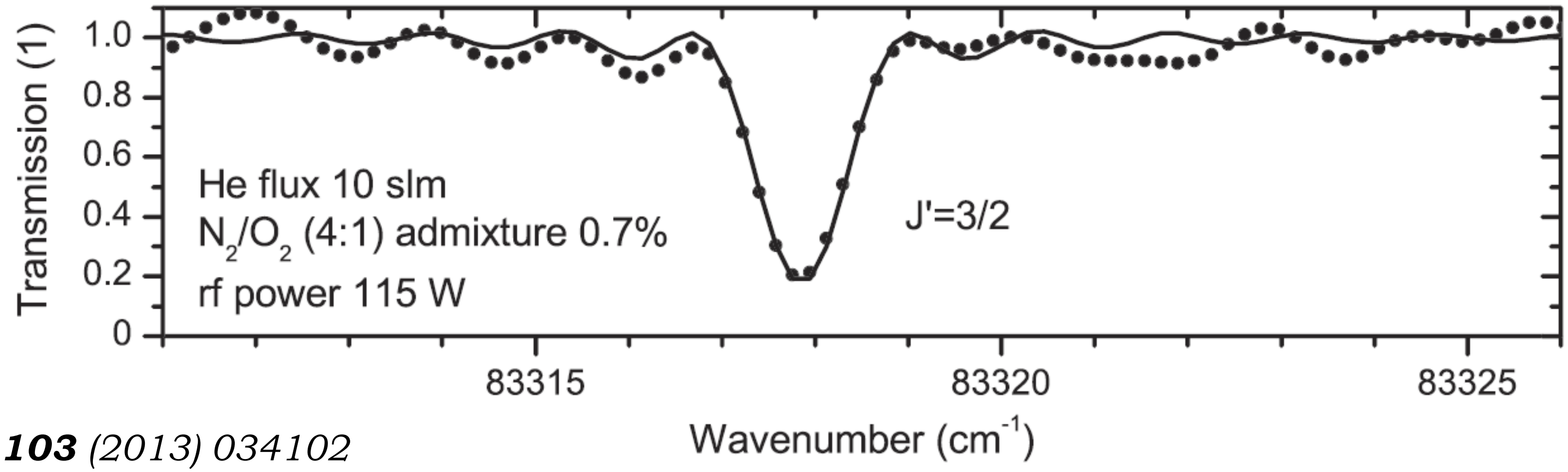

*Niemi et al. APL **103** (2013) 034102*

Modeling of microplasmas

- Difficulty of diagnostics → considerable emphasis on numerical modeling

- Different kind of model: PIC, fluid and global

RF capacitive discharges at atmospheric pressure (APPJ)

V. Schulz-von der Gathen *et al.*, J. Phys. D **41** (2008) 194004

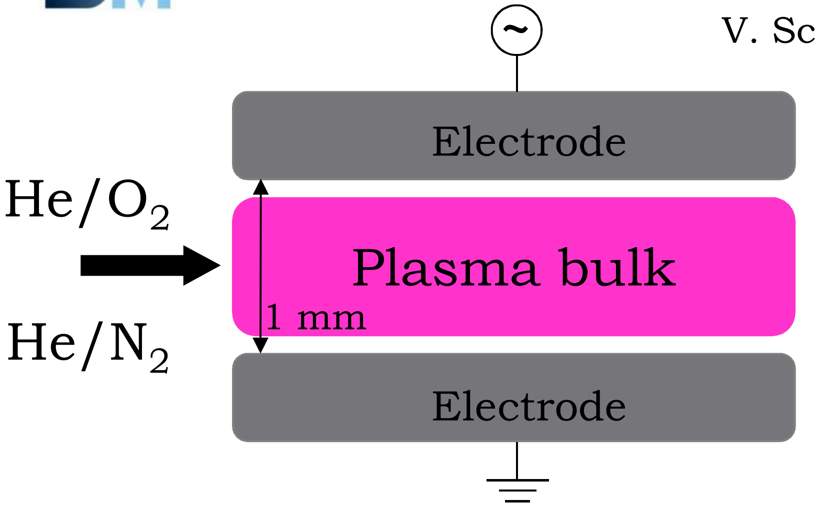

- RF frequency : 13.56-27.12 MHz
- electrode gap :1 mm
- He/O_2 or He/N_2
- Gas flow to produce the plasma jet

- 1D PIC simulation in He/N_2

(Kawamura *et al.* PSST **23** (2014) 035014)

- 1D Fluid model in He/O_2

(Niemi *et al.* PSST **20** (2011) 055005)

- Global model in He/N_2 and He/O_2

(Lazzaroni *et al.* PSST **21** (2012) 035013)

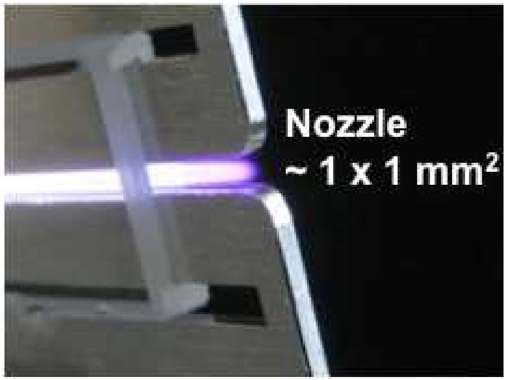

Plasma kinetic description

- Particle-in Cell (PIC) simulations: Define macro-particle and solve the motion of each of these self-consistently with the fields. Method based on Newton's laws. Calculation of the electric field at every time-step from positions of charged particles (Poisson equation)
- Collisions are treated with Monte Carlo (MC) approach
- Advantage: accurate and self-consistent approach; fields, particle densities and fluxes obtained without making any assumptions about the particle temperatures or velocity distribution
- Disadvantage: long calculation time, no or simple chemistry

PIC-MCC simulation of APPJ

- RF-APPJ in He/0.1%N_2 (electropositive plasma); 1D simulation
- Each computer particle represents a cluster of 10^7 “real” particles

For each timestep:
1) Particles are linearly weight → charge density at the grid points
2) Poisson’s equation → electric field at the grid points
3) Determination of the force on each particle
4) Motion Newton equation → particle new positions and velocities
5) Boundaries conditions → bound particles are removed and injected particles are introduced (secondary electrons)
6) MCC handler → collisions → particle velocities are adjusted

3 species: N_2^+, He* and e^-
8 collisions

Time calculation ~ day

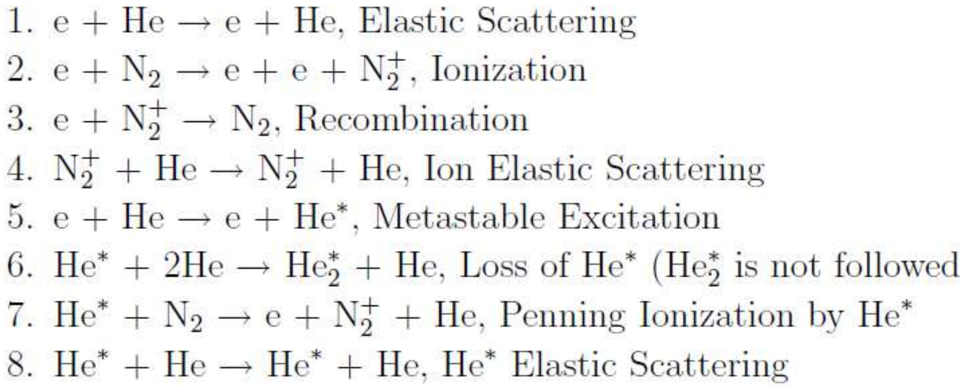

1. $e + He \rightarrow e + He$, Elastic Scattering
2. $e + N_2 \rightarrow e + e + N_2^+$, Ionization
3. $e + N_2^+ \rightarrow N_2$, Recombination
4. $N_2^+ + He \rightarrow N_2^+ + He$, Ion Elastic Scattering
5. $e + He \rightarrow e + He^*$, Metastable Excitation
6. $He^* + 2He \rightarrow He_2^* + He$, Loss of He^* (He_2^* is not followed
7. $He^* + N_2 \rightarrow e + N_2^+ + He$, Penning Ionization by He^*
8. $He^* + He \rightarrow He^* + He$, He^* Elastic Scattering

PIC simulation of APPJ

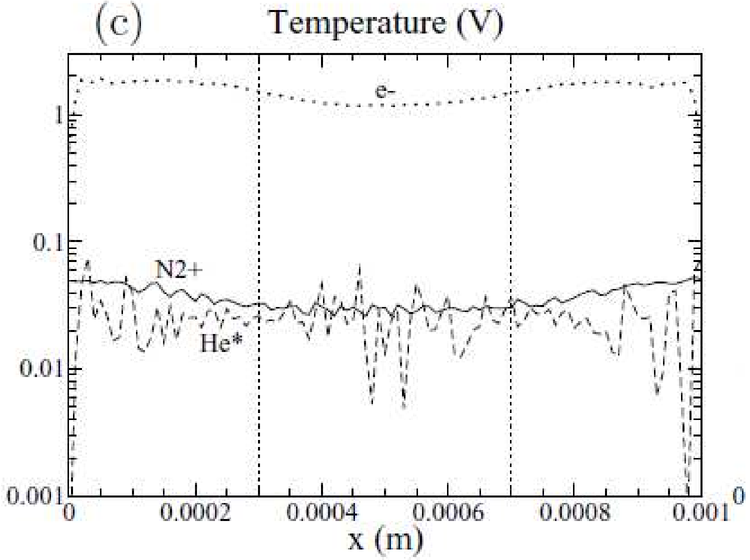

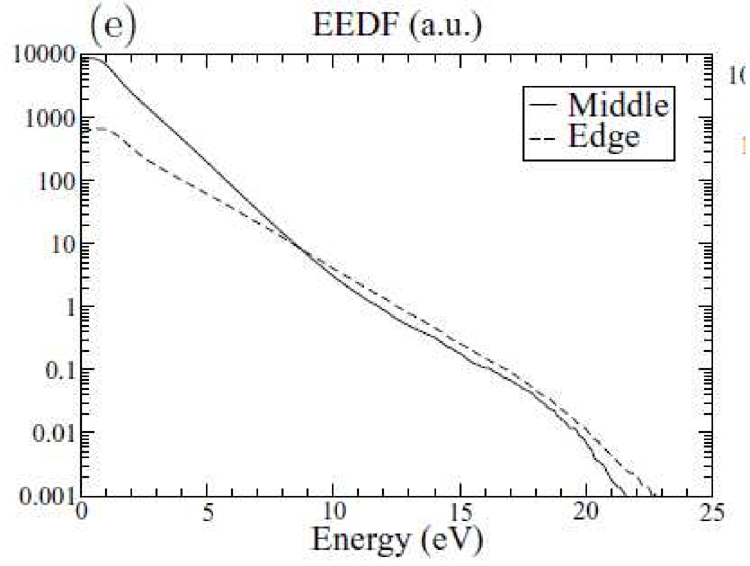

f = 27.12 MHz

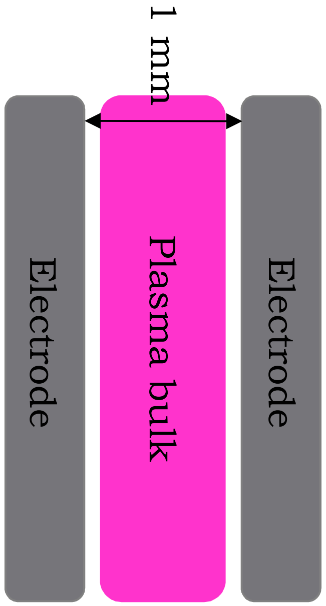

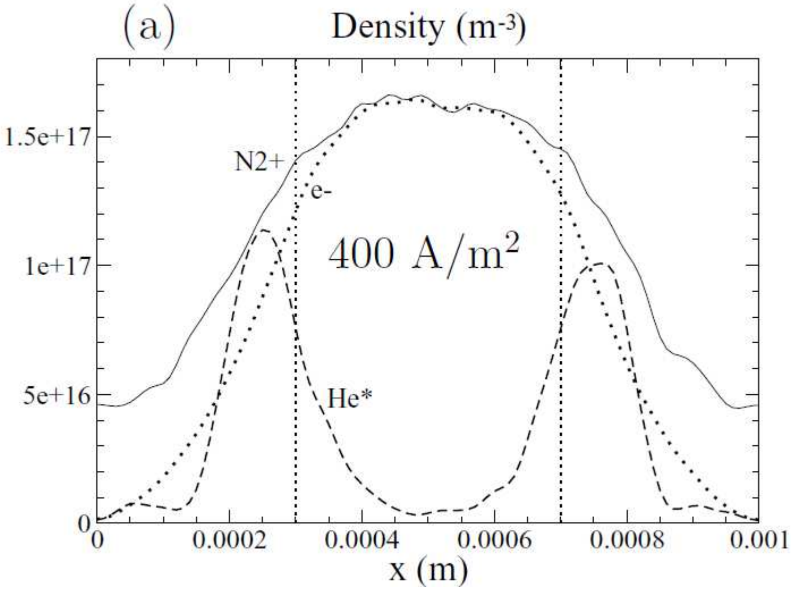

f = 13.56 MHz

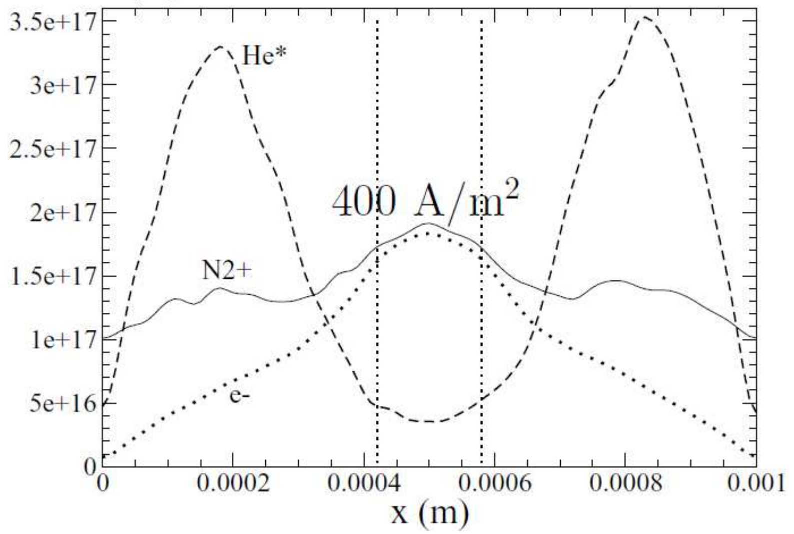

Fluid description

- Particle conservation equation or continuity equation (obtained by integrating the Boltzmann equation over velocity space):

$$\frac{\partial n}{\partial t} + \nabla \cdot (n\mathbf{u}) = S - L$$

volume source term

volume loss term

- Momentum conservation equation (obtained by integrating the Boltzmann equation over velocity space after multiplication by mv), with B=0:

$$nm\left[\frac{\partial \mathbf{u}}{\partial t} + (\mathbf{u} \cdot \nabla)\,\mathbf{u}\right] = nq\mathbf{E} - \nabla p - m\mathbf{u}\,[n\nu_{\mathrm{m}} + S - L]$$

- Energy conservation (obtained by integrating the Boltzmann equation over velocity space after multiplication by 0.5mv^2)
- Coupled to Poisson equation for self-consistent E field
- Can be coupled to a Boltzmann's solver for accurate rate coefficient

Fluid model of APPJ

He/O_2
(electronegative plasma)

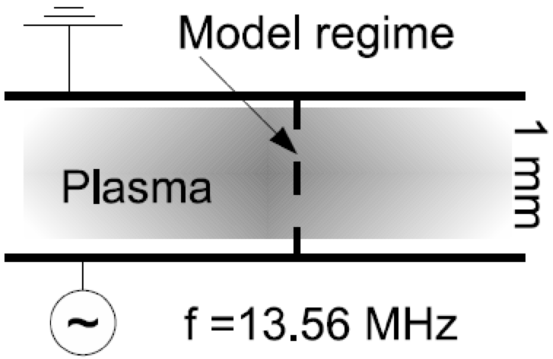

- Importance of electron dynamics
- Electron power strongly non uniform in space and time
- 1D fluid model

Spatio-temporal simulated electron-impact excitation of helium into the metastable state He

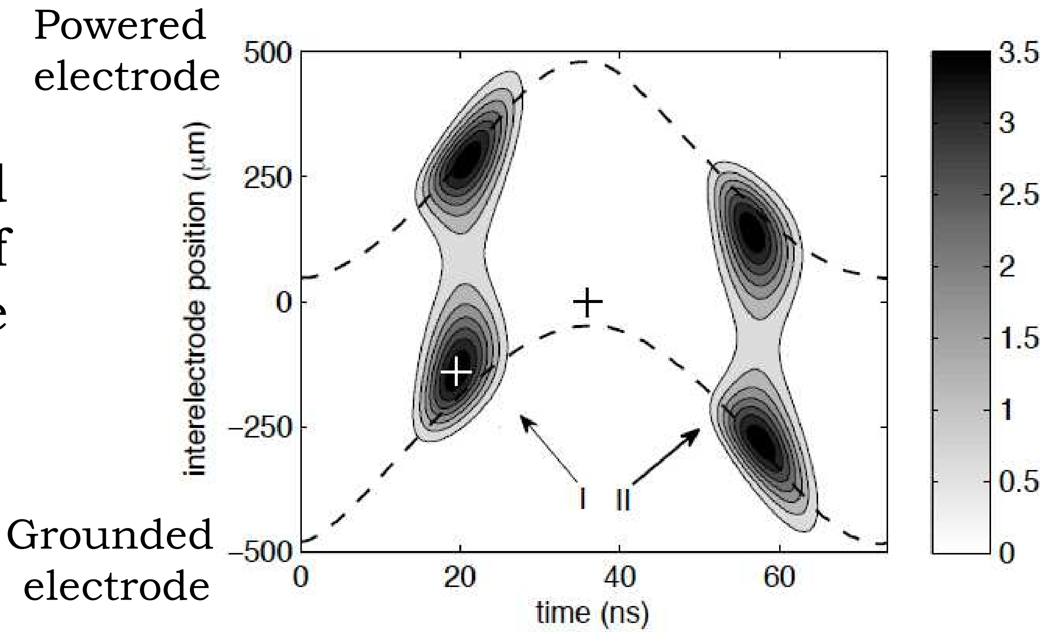

low power operation at 0.6 W/cm^2

16 species
116 reactions

Time calculation ~ few hours

Fluid model of APPJ

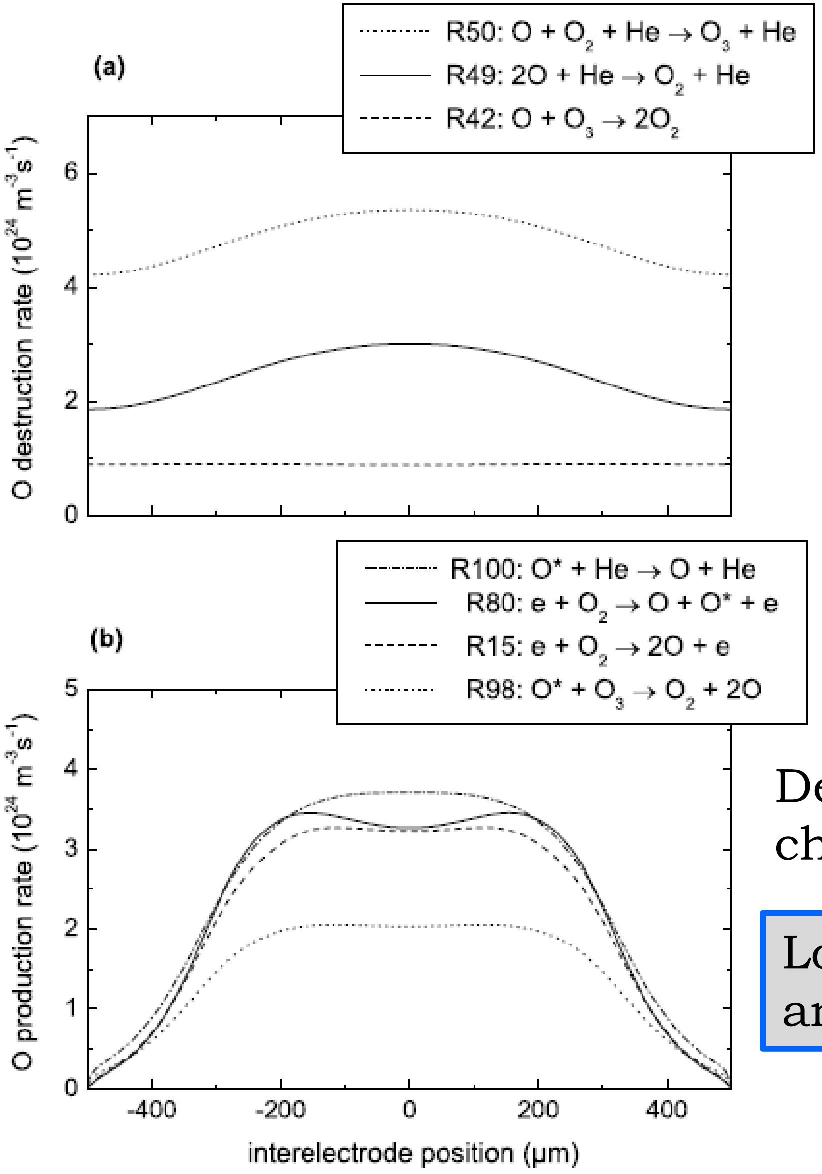

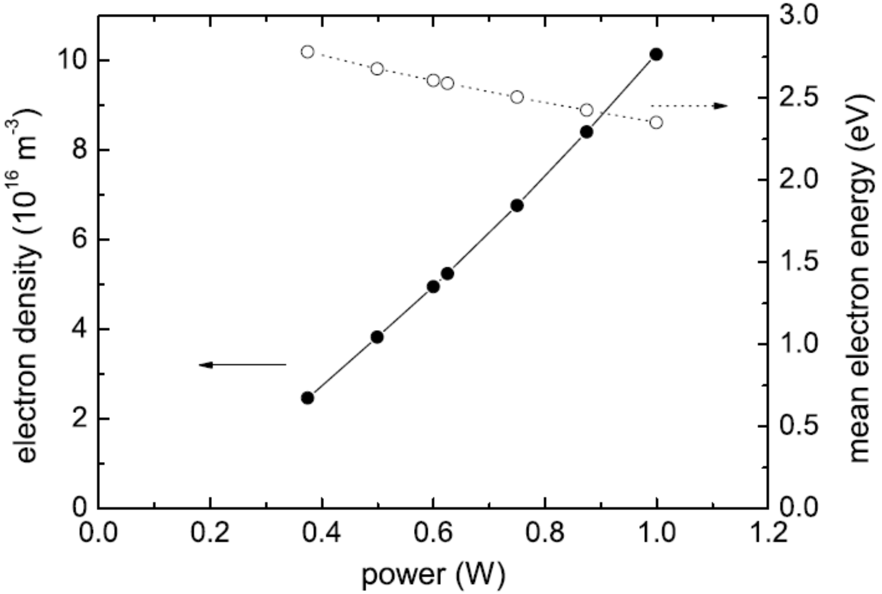

Time and space averaged electron density and mean electron energy

Decrease of n_e and increase of T_e with power; change in the time and space averaged EEDF

Lost of accuracy but faster calculation time and more complexe chemistry than PIC model

Global description

- Volume-averaged (0D) model: densities and temperatures are uniform in space (obtained by spatial integration of fluid equations)

- Particle balance: $$\frac{dn_\alpha}{dt} = G_\alpha - P_\alpha$$

- Electron power balance:

$$\frac{d}{dt}\left(\frac{3}{2}n_e e T_e\right) = P_{\text{abs}} - P_{\text{dis}}$$

Particle balance at low pressure

- Particle losses at the walls. The term P_α contains volume and wall losses. For the electron particle balance at low pressure, wall losses dominate and in one dimension:

$$\frac{d\overline{n}_e}{dt} = \overline{n}_e n_g K_{iz} - \frac{2\Gamma_{wall}}{l}$$

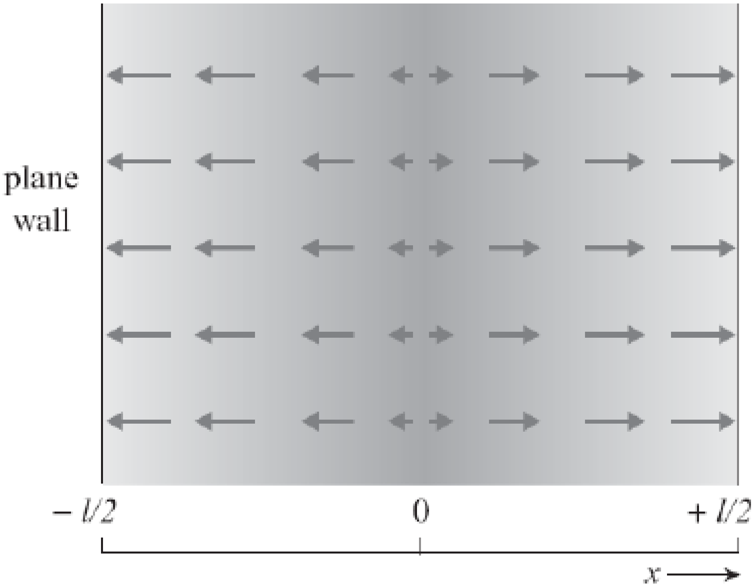

- A plasma transport theory is required to relate the space-averaged electron density to the flux at the wall

Particle balance: issues in µplasmas

- In microdischarges, ionization is often non uniform. Classical low-pressure transport theory do not apply
- Fortunately in some instances volume losses dominate (recombination)
- However, evaluation of wall losses is a critical point for high-pressure discharges modeling
- Properly evaluate the reaction rates ($T_e(x,t)$)
- Properly evaluate the electron power absorption

Hybrid analytic-numerical global model of APPJ

→ Fast solution of the discharge equilibrium: exploration of a large parameter space

→ Variations of discharge parameters with discharge composition and RF power

Homegeneous discharge model

Principles of Plasma Discharges and Materials Processing, M.A.Lieberman and A.J.Lichtenberg, 2nd Edition, John Wiley and Sons Inc., New York, 2005
Physics of Radiofrequency Plasmas, P. Chabert and N. Braithwaite, Cambridge University Press, 2011

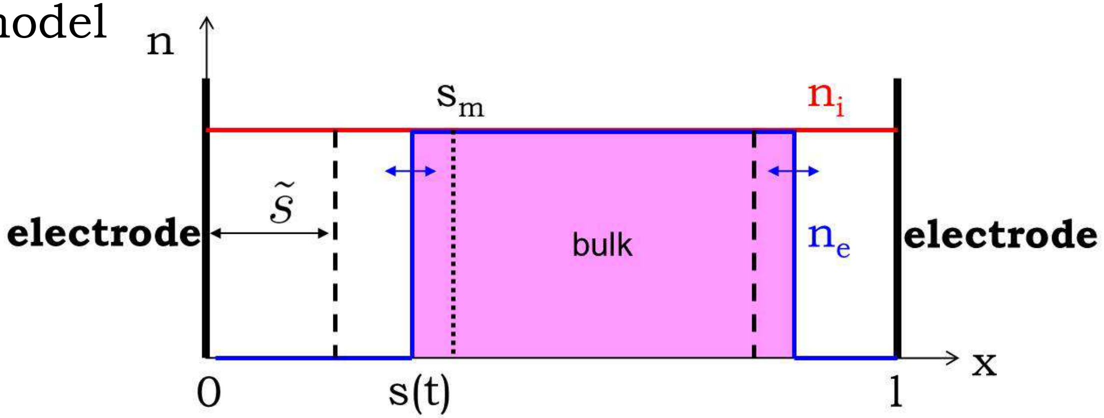

- Three regions: - a quasi-neutral plasma ($n_i=n_e=n_0=$const)
  - two sheaths ($n_i=n_0$ and $n_e=0$)
- Ions do not respond to the RF field
- Analytical expressions of $J_C(t)$, s(t), E(t) and $P_C(t)$

Global model

Particle balance / Global e⁻ power balance

$$\boxed{\frac{dn_\alpha}{dt} = G_\alpha - P_\alpha}$$

$$\boxed{\frac{\mathrm{d}T_\mathrm{e}}{\mathrm{d}t} = \frac{2}{3}\frac{P_\mathrm{c}(t)}{en_\mathrm{e}} - \frac{2}{3}\nu\frac{3m}{M}T_\mathrm{e} - \sum_j \frac{2}{3}\nu_j\mathcal{E}_j}$$

numerically

analytically

3) Mean rate coefficient

1) $P_c(t)$ ← homogeneous discharge

2) $T_e(t)$ ← analytical integration

$$\Downarrow$$

Discharge equilibrium

Electron temperature

Electron energy balance: $$\frac{\mathrm{dT}_e}{\mathrm{d}t} = \frac{2}{3}\frac{P_\mathrm{c}(t)}{e n_e} - \frac{2}{3}\nu\frac{3m}{M}\mathrm{T}_e$$

$$\boxed{P_\mathrm{c}(t) = \overline{P}_\mathrm{c}[1 + \cos(2\omega t - \theta)]}$$

Hypothesis: -T_e(t) uniform in the bulk
-n_e uniform and independant of time

↓ integration

$$\boxed{\mathrm{T}_e(t) = \overline{\mathrm{T}}_e + \widetilde{\mathrm{T}}_e\cos(2\omega t - \phi_0)}$$

Electron temperature

$$\boxed{\mathrm{T}_e(t) = \overline{\mathrm{T}}_e + \widetilde{\mathrm{T}}_e \cos(2\omega t - \phi_0)}$$

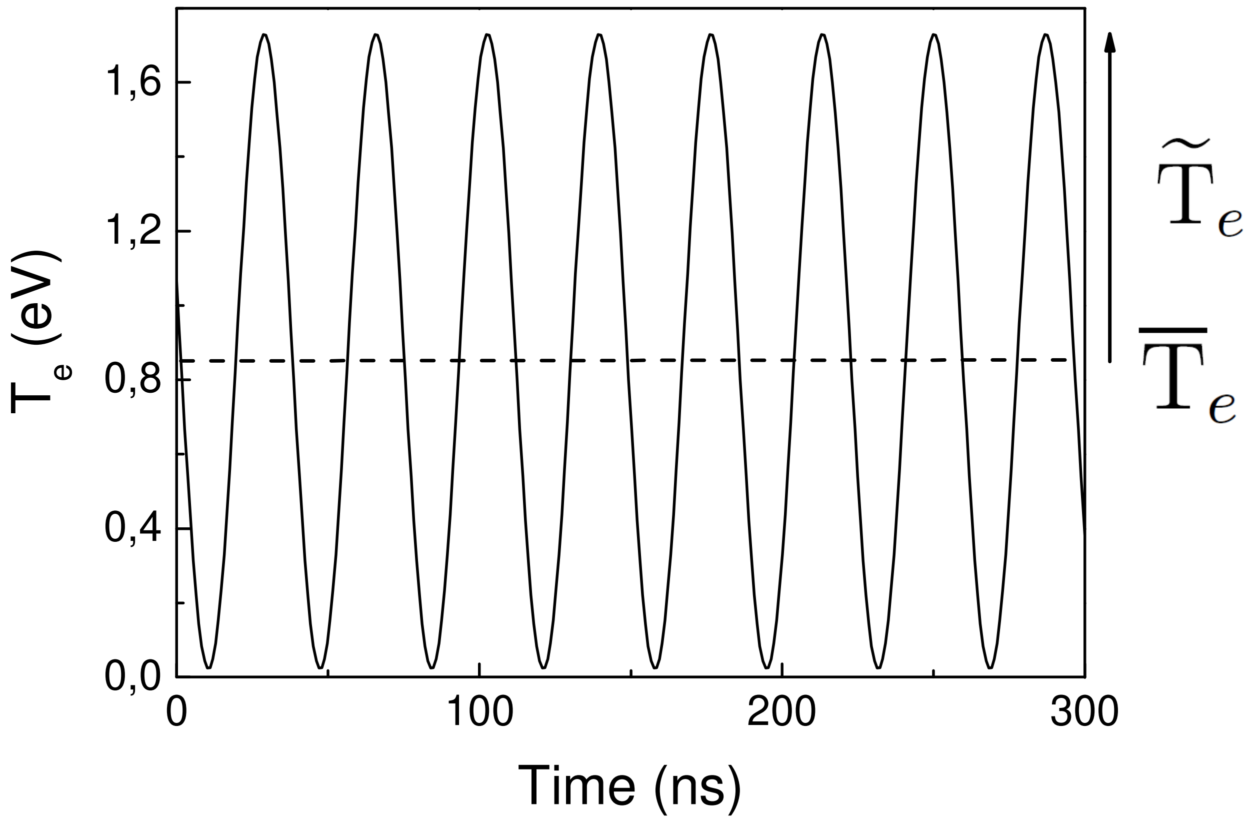

Unlike at low pressure, Te oscillates during the rf cycle. This point is extremely important for the global modeling.

Effective rate coefficients

- Electron-activated processes strongly affected by $T_e(t)$
- Maxwellian rate coefficients: $K = K_0 \exp(-\mathcal{E}_a/\mathrm{T}_e)$
- Averaging over the oscillating T_e

→ enhanced rate coefficient:

$$\boxed{\overline{K} = K_0(\mathrm{T}_{emax})\,\mathrm{erfc}\left(\sqrt{\mathcal{E}_a/2\widetilde{\mathrm{T}}_e}\right)}$$

$$\langle K_0 \exp\left(-E_a/T_e(t)\right)\rangle \neq K_0 \exp\left(-E_a/\left\langle T_e(t)\right\rangle\right)$$

Particle balance: He/N_2 chemistry

Particle balance for each species:

$$\frac{dn_\alpha}{dt} = G_\alpha - P_\alpha$$

Electropositive plasma He-N_2 mixture

- 0.1% of N_2
- 8 species
- 15 reactions in the gas phase
- Surface reactions for all species
- Tg=345 K

The 8 species:

He, He^+, He_2^+, He^*,
He_2^*, N_2, N_2^+ and e^-

Time calculation ~ few ms

Particle balance: He/O_2 chemistry

Particle balance for each species:

$$\frac{dn_\alpha}{dt} = G_\alpha - P_\alpha$$

Electronegative plasma He-O_2 mixture

- 0.1-1 % of O_2
- 16 species
- 132 reactions in the gas phase
- Surface reactions for all species
- Tg=345 K

The 16 species:

He, He^+, He_2^+, He*, He_2^*, O_2, O, O_3, O^+, O_2^+, O^-, O_2^-,O_3^-, O*, O_2* and e^-

Time calculation ~ few seconds

Sheath physics: limitation in %O_2

- Finite sheath widths limit operating regimes in atmospheric pressure discharges.
- Requirement for equilibrium: $\bar{s} < l/2$
- Time average energy balance and magnitude of the oscillating sheath width give ($\nu >> \omega$):

$$\omega\bar{s} = u_{Bg}(6\bar{\zeta})^{1/2}$$

$$u_{Bg} = (e\overline{T}_{\mathrm{e}}/M)^{1/2}$$

RF time average energy loss factor

Sheath physics: limitation in $\%O_2$

- Sheath size increases with $\%O_2$
- Limit of $\%O_2$ when sheath size exceeds half-gap

$$\omega \bar{s} = u_{Bg}(6\bar{\zeta})^{1/2}$$

- The RHS increases with the O_2 fraction (inelastic collisions)

- Requirement for equilibrium: $\bar{s} < l/2$

- Therefore there is a limit $\%O_2$ at given frequency

- Higher possible $\%O_2$ at higher frequency

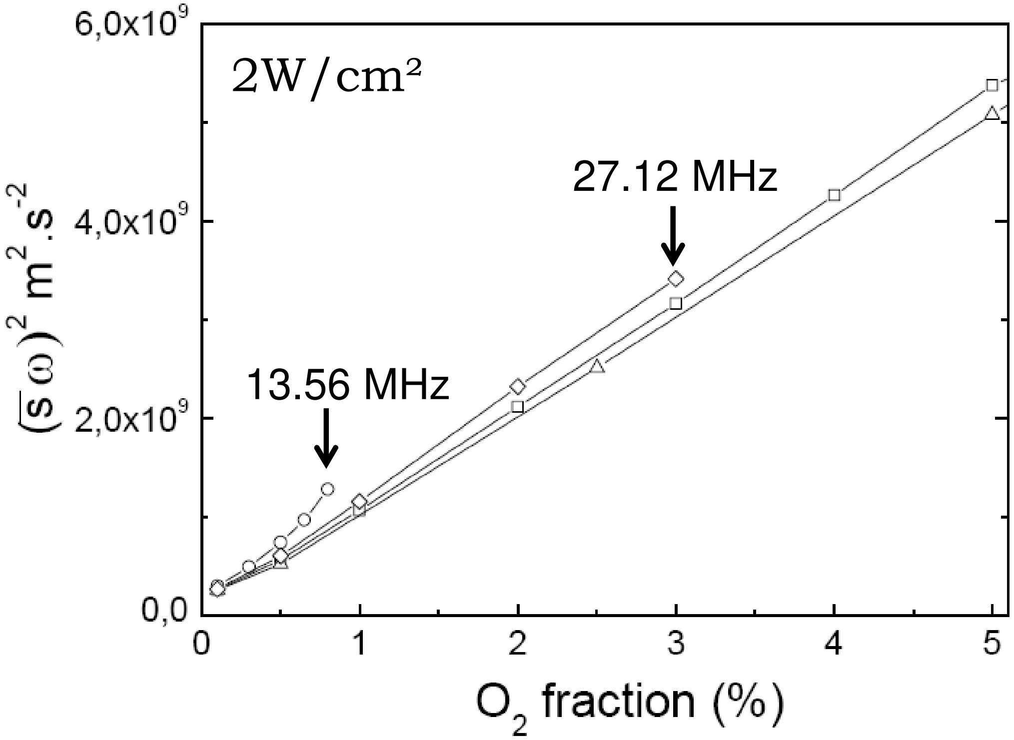

$$\boxed{\mathrm{O}_{2\mathrm{Lim}}\% \approx 1.3\left(\frac{l(\mathrm{mm})f(\mathrm{MHz})}{13.56}\right)^2}$$

Global model vs PIC simulation

He/N_2

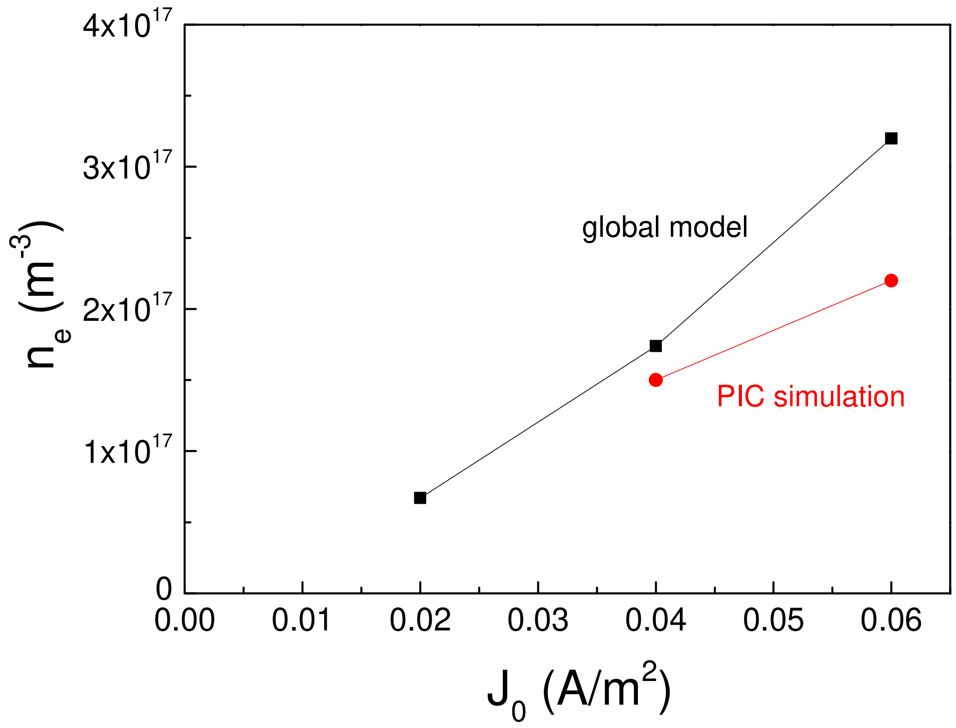

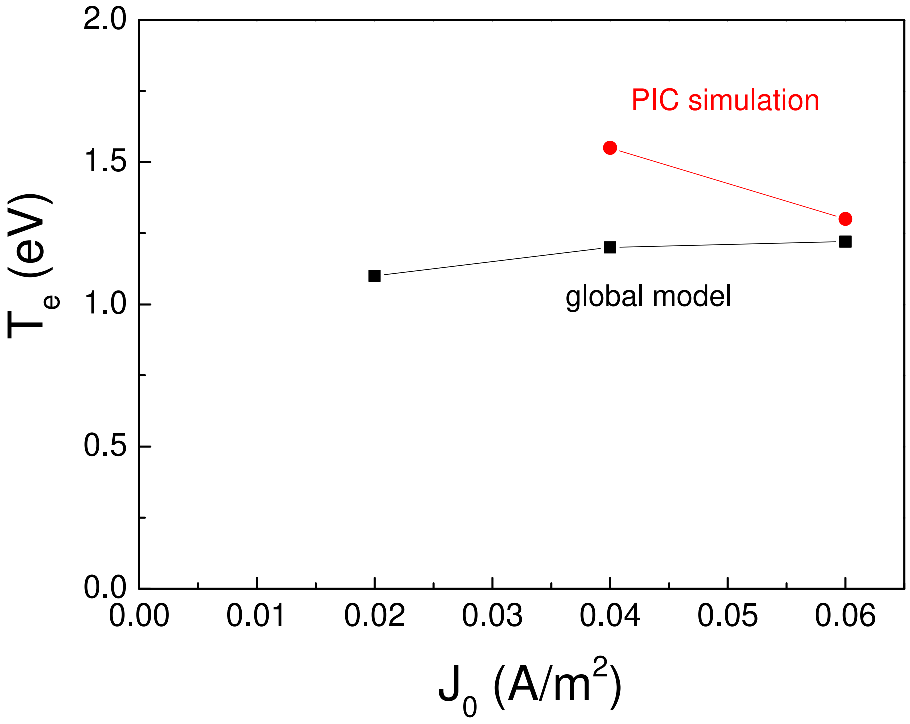

Global model vs fluid model: neutral species

He/O_2

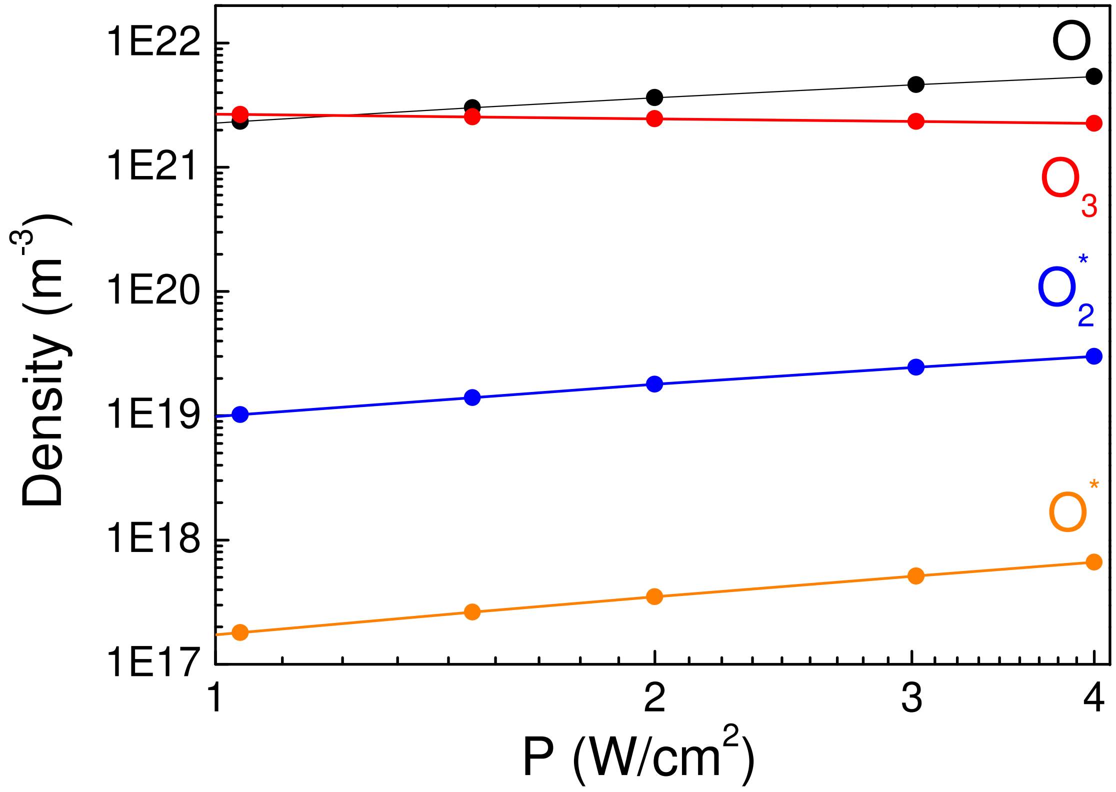

Global model vs fluid model: neutral species

He/O_2

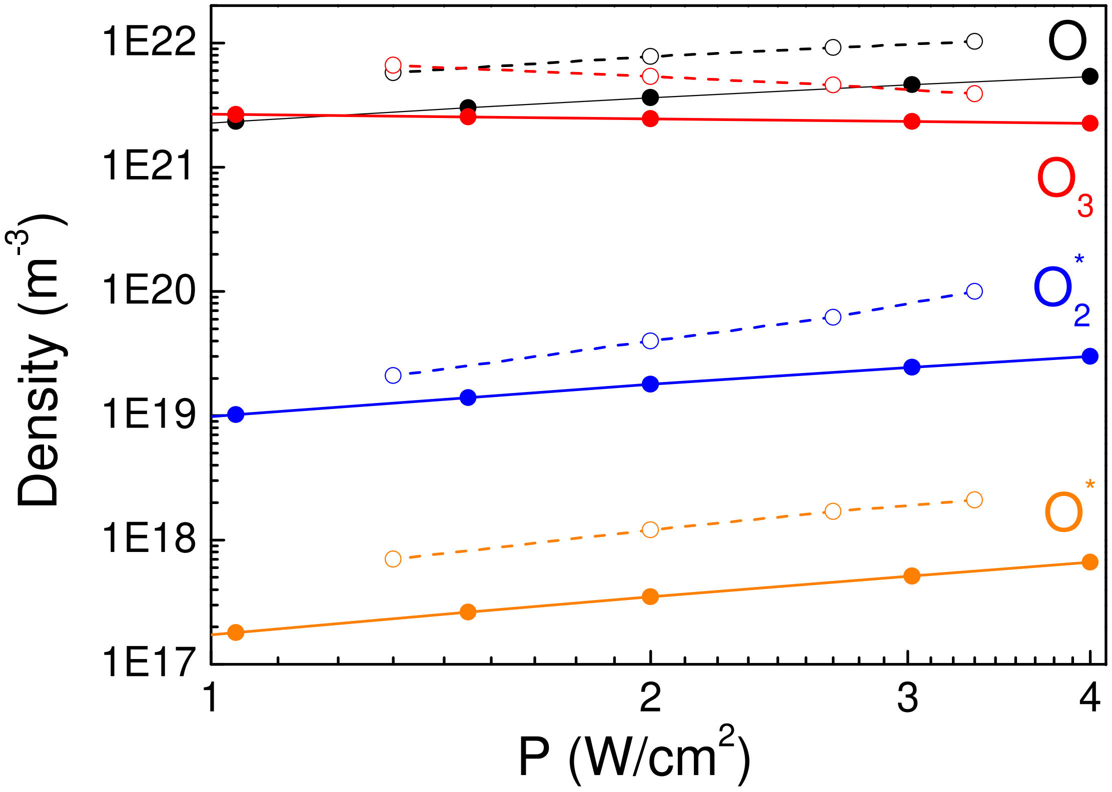

Global model → lines
Fluid model → dash lines

- Good qualitative agreement

- Global model predictions lower than that of fluid model (factor of 2 for O and O_3 and factor of 3 for O^* and O_2^*)

Global model vs fluid model: charged species

He/O_2

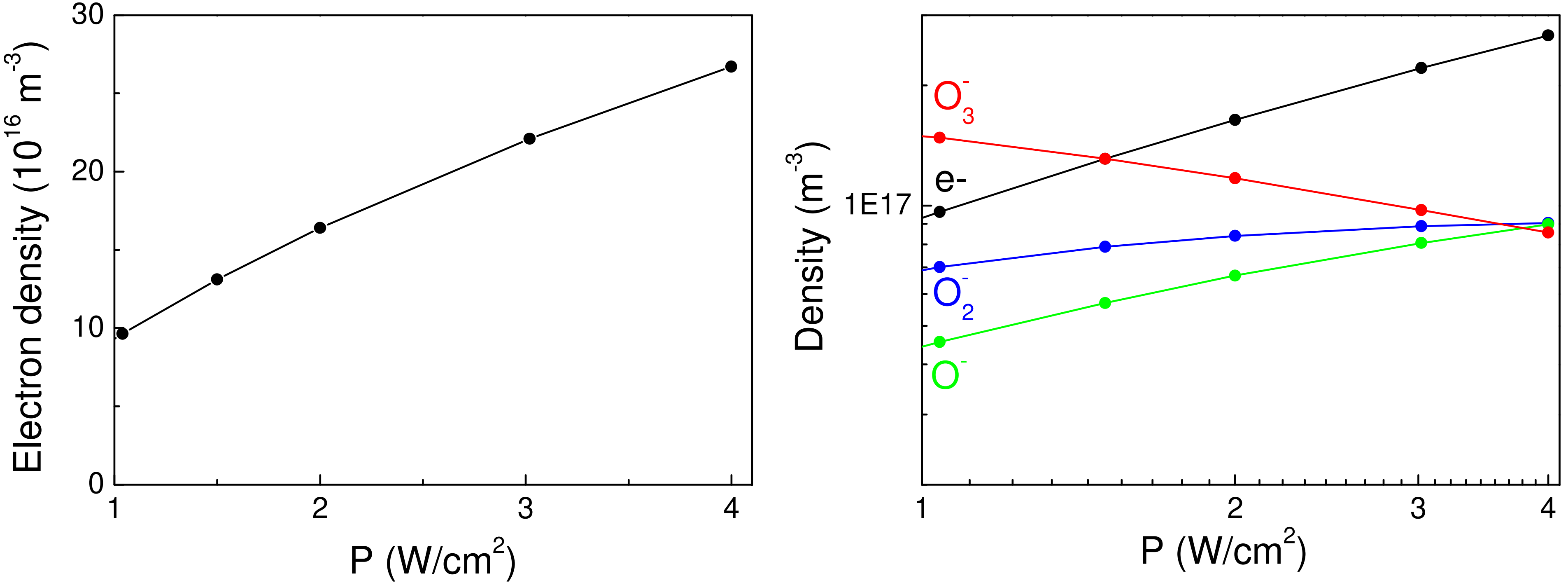

Global model vs fluid model: charged species

Global model → symbols + lines
Fluid model → open symbols + dash lines

He/O_2

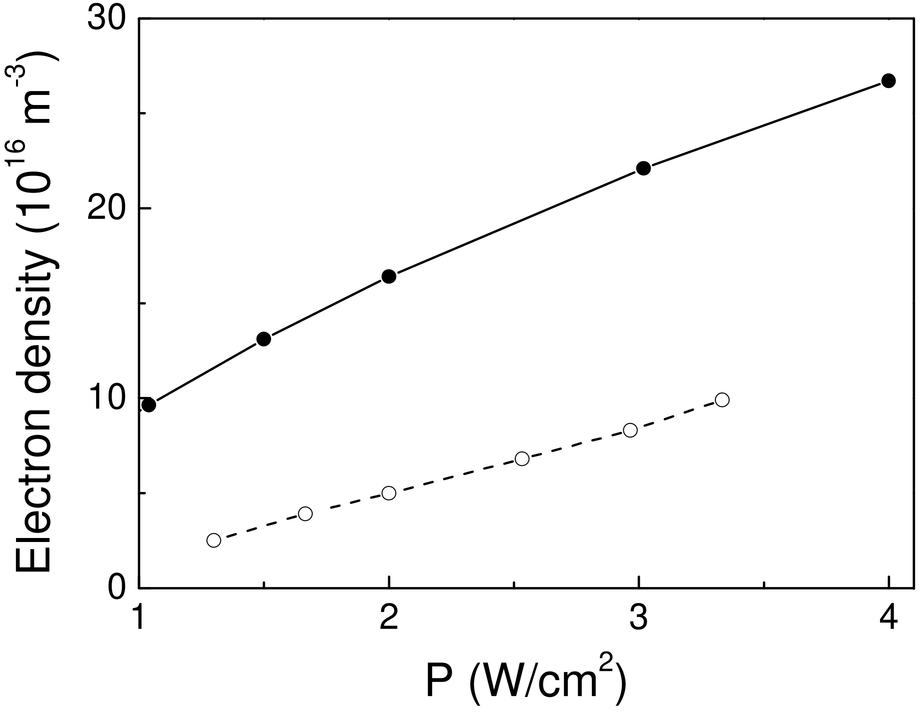

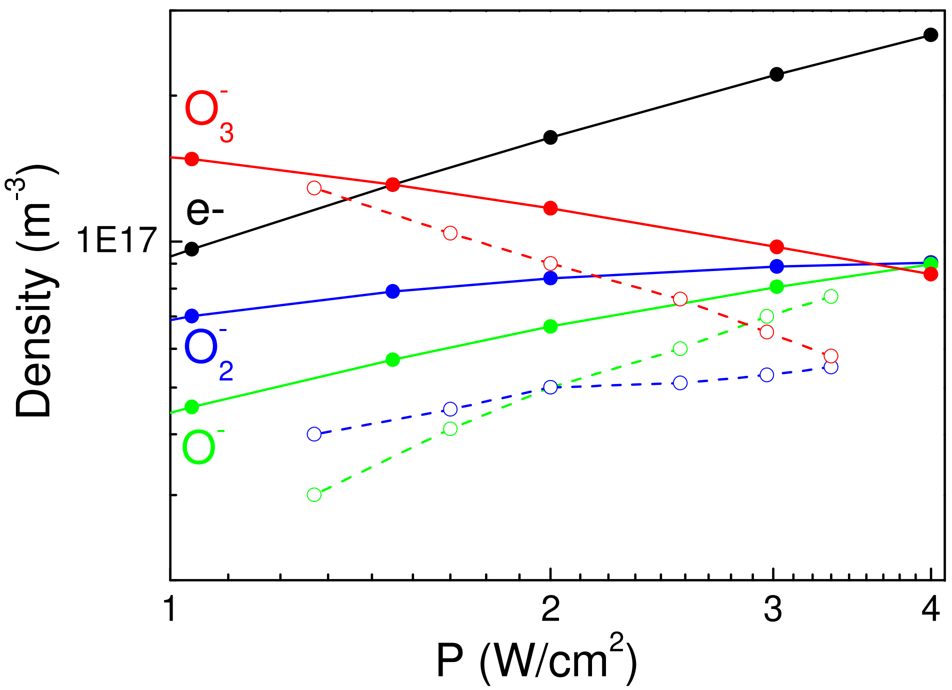

- Good qualitative agreement
- n_e (global model) ≈ 3*n_e (fluid model)
- Negative ion densities (global model) ≈ 3/2*Negative ion densities (fluid model)

Hybrid model

- Some species are fluid-like and others are particle-like → hybrid model
- PIC-MC for particles which need detailed distribution function (often electrons in μplasmas)
- Fluid model for others species (often ions and neutrals)
- Advantages: accurate + self-consistent + reduced calculation time

Hybrid model: example

- Hybrid model of a MHCD in Ar (hole diameter = 200-300 μm)
- 2D fluid model + MC simulation for beam electrons emitted at the cathode

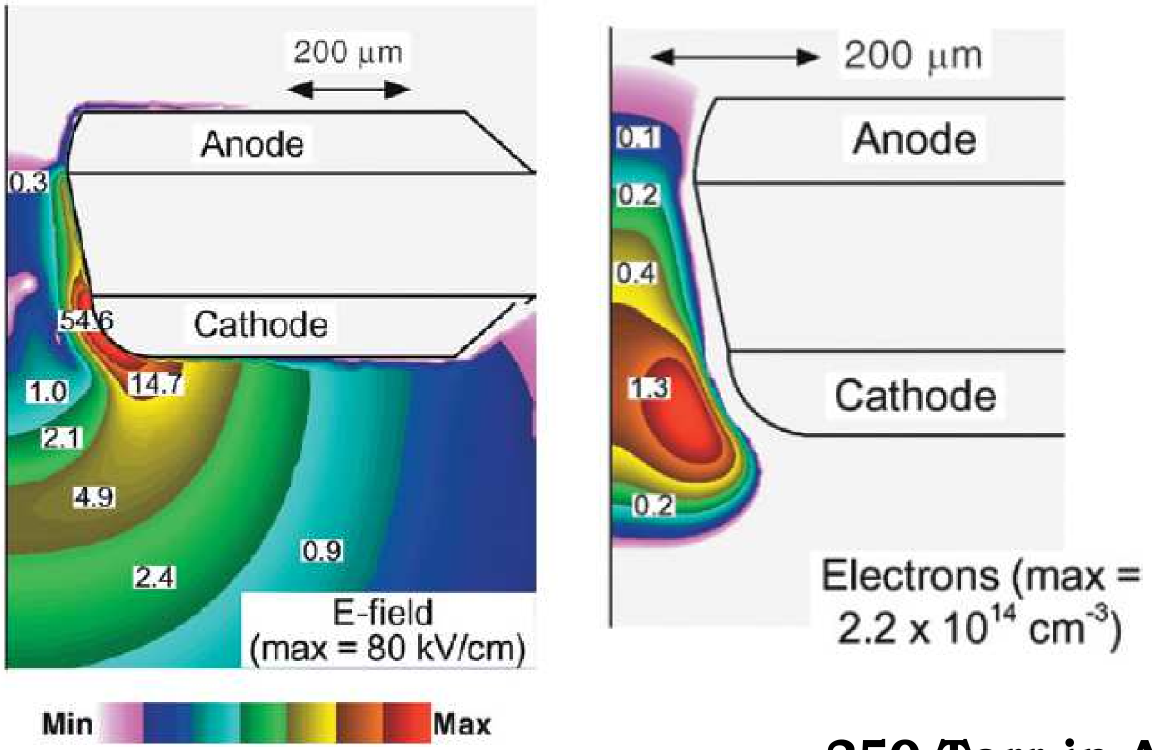

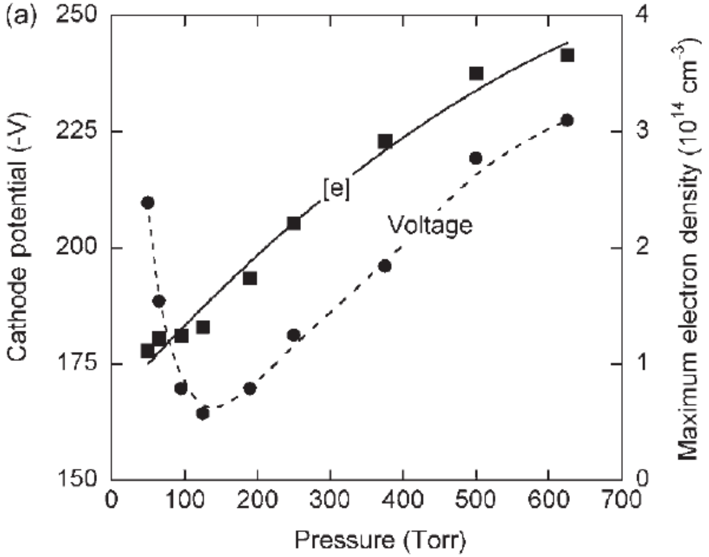

250 Torr in Ar with I = 2 mA

Kushner, JPhysD ***38*** *(2005) 1633*

Microplasmas for material synthesis

- Synthesis from vapour precursors
- Synthesis from evaporation or sputerring of a sacrificial electrode
- Synthesis from plasma-liquid interactions

Synthesis from vapour precusors: exemple of bimetallic nanoparticles Ni_xFe_{1-x}

*Chiang et al., Advanced Materials **20** (2008) 4857, USA*

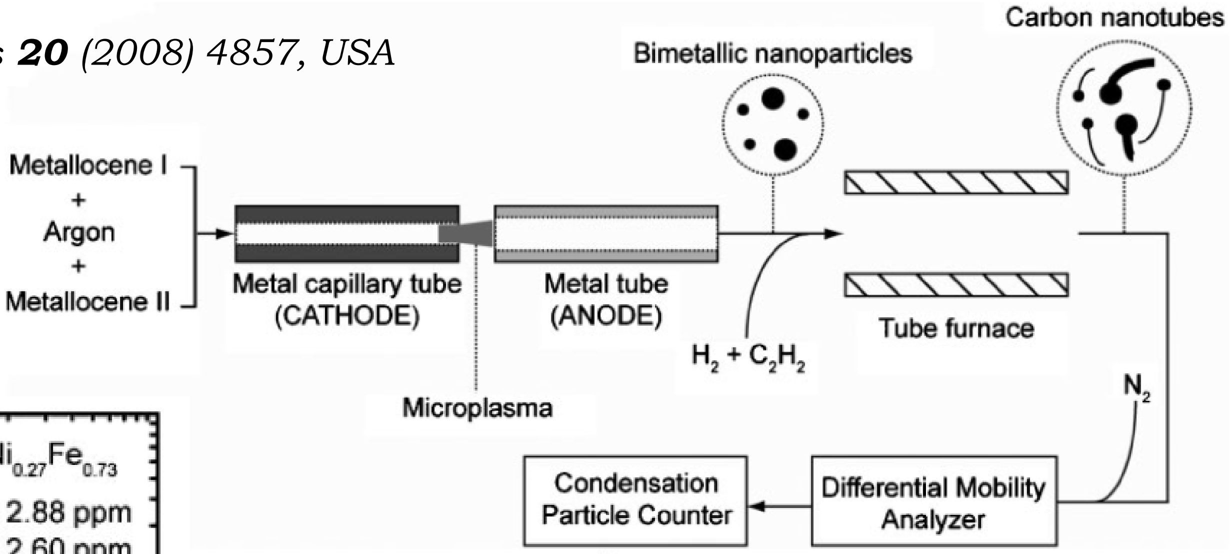

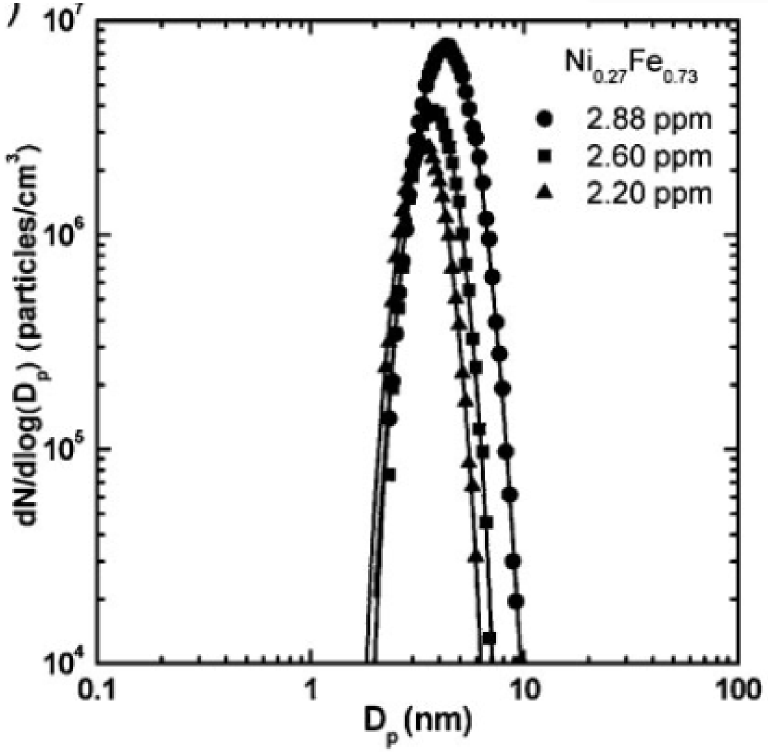

Growth of carbon nanotubes at Patm
Cathode diameter =180 µm
DC power
Electrode gap = 1 mm
I = 7 mA; V= 400 V

Size distributions
(differential mobility analyser)

Synthesis from evaporation/sputtering of solid metal electrodes

Mariotti et al., IEEE Trans. Plasma Sci. ***37*** *(2009) 1027, UK*

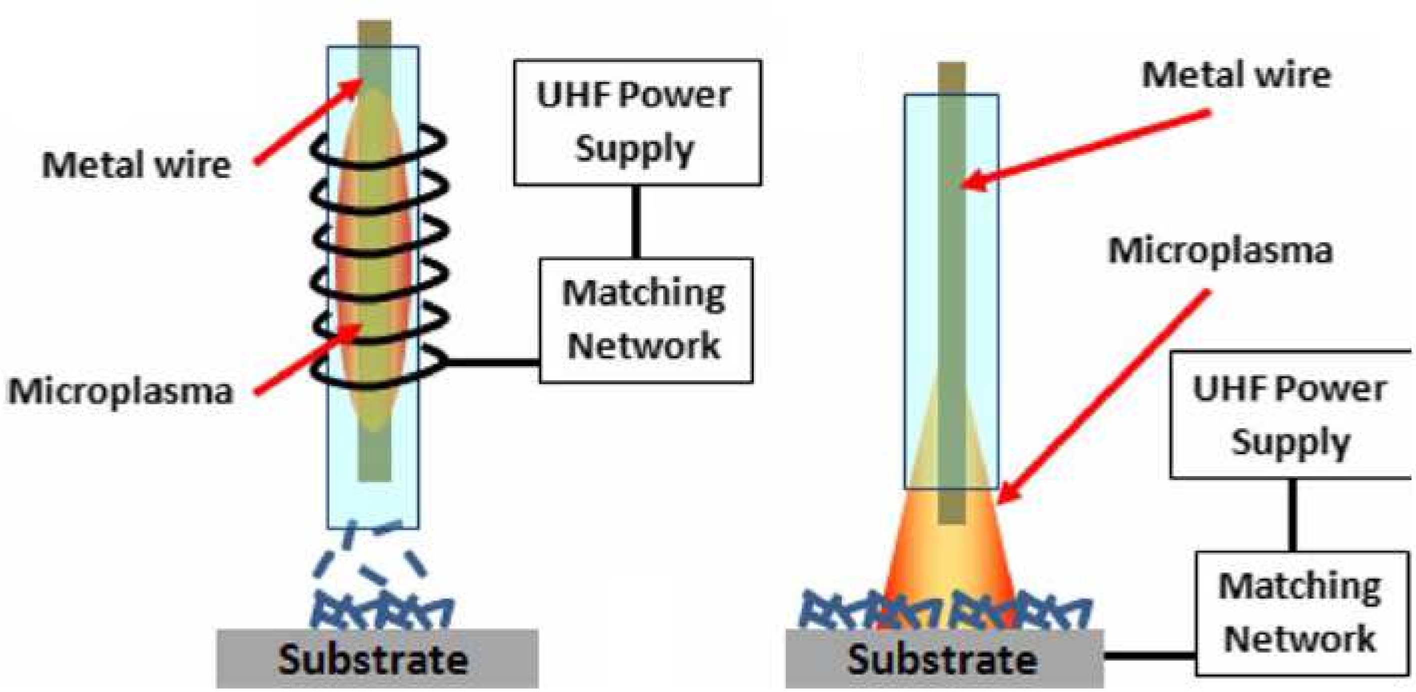

Remote fabrication

Microplasma in direct contact with the processing surface

Synthesis of metal and metal-oxide nanostructures

Deposition of ZnO thin films by inductively coupled microplasmas

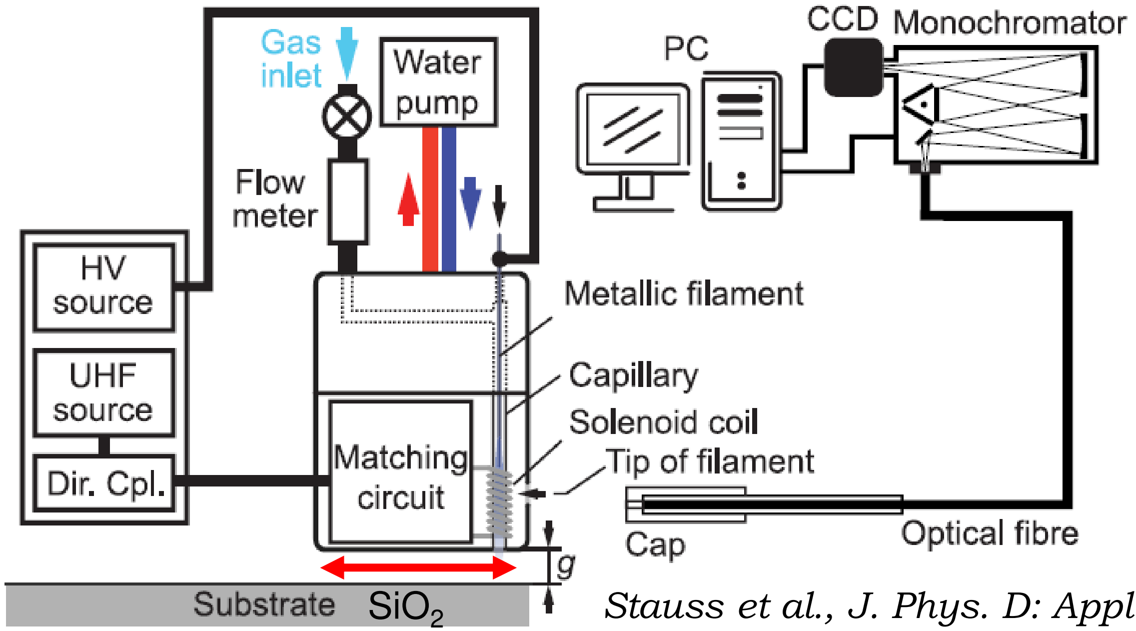

-Thin filament in quartz capillary
-Zn finament diameter: 0,25 mm
-Ignition:short HV dc (0,5s;15 kV)
-Plasma sustained by a solenoidal coil (UHF generator, f=450 MHz)
-Patm, Ar gas (50-200 sccm), 25W

Stauss et al., J. Phys. D: Appl.Phys. ***43*** *(2010) 155203, Japan*

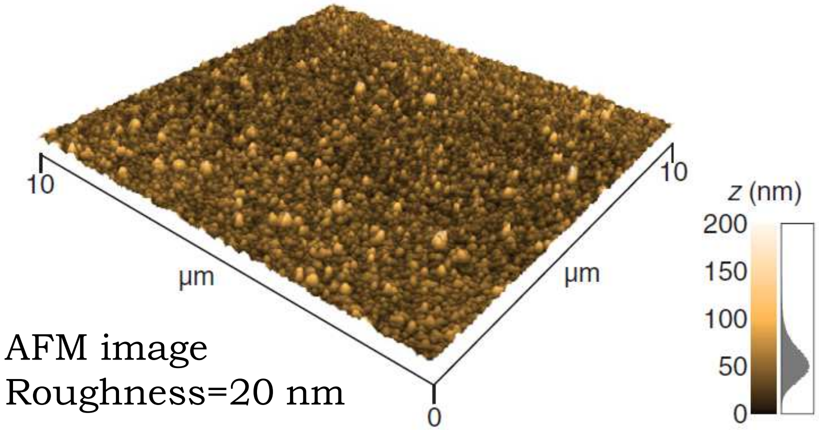

AFM image
Roughness=20 nm

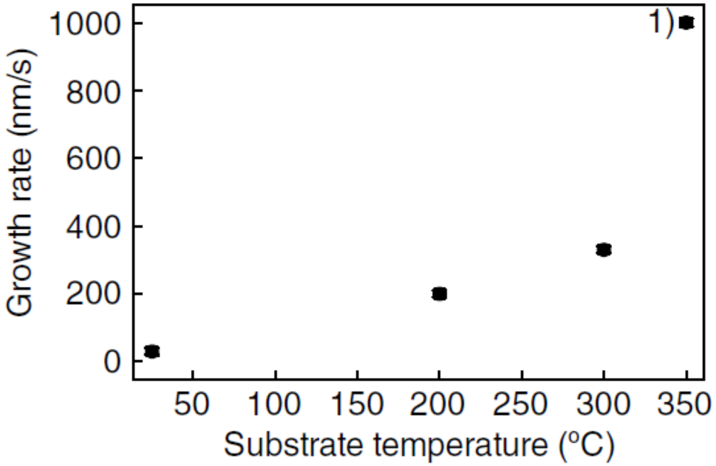

Synthesis of Si nanocones by RF microplasma

*Yang et al., Thin solid films **515** (2007) 4158 , Japan*

-Atmospheric pressure
-Ar/CH_4 mixture
-flow rate: 10-50 sccm
-distance electrode-substrate: 3 mm
-RF power = 35 W

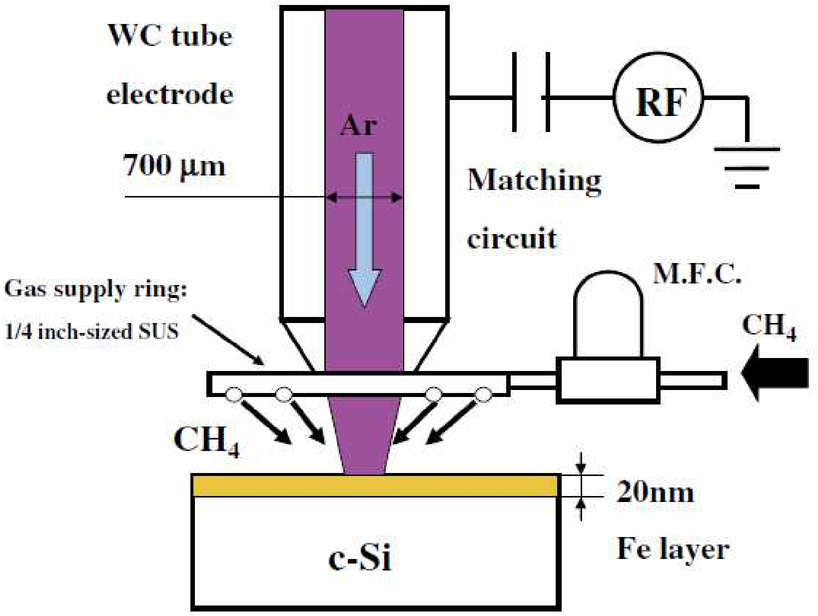

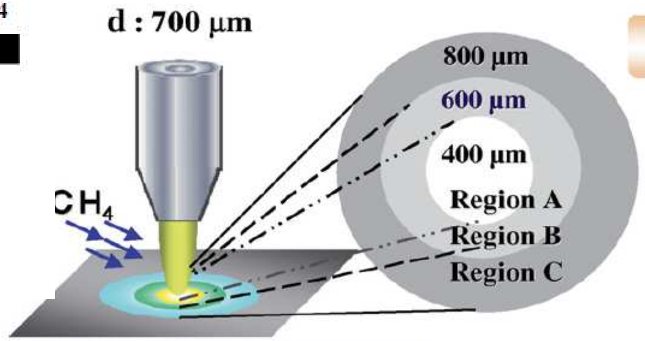

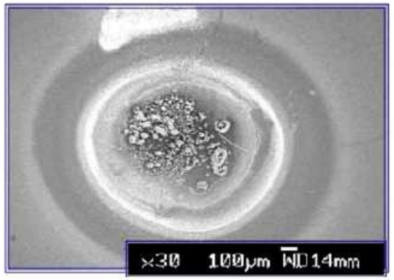

SEM image of products formed underneath the tube electrode

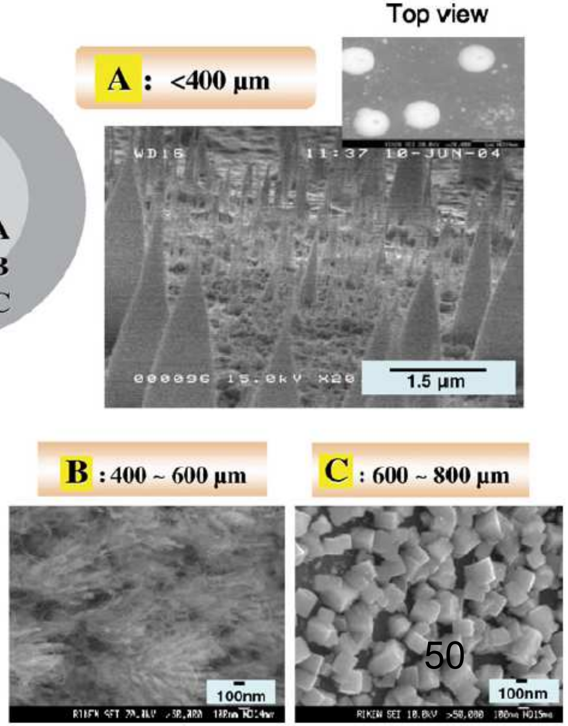

Region A: cone-shaped products (Si)
Region B: nanowire structures (C)
Region C: cubic-shape products (tungsten oxide WOx and diamond particles)

Synthesis by plasma-liquid interactions: example of Ag nanoparticles (SERS)

Chang et al., J. Vac. Sci. Technol. ***28*** *(2010) L5, USA*

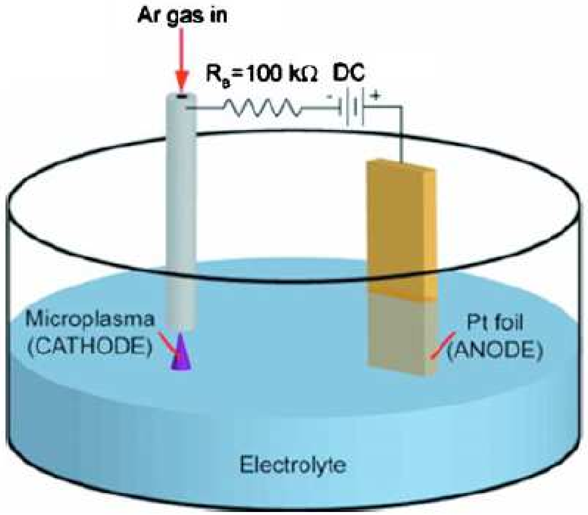

-Anode: Pt, 1 cm x 1 cm
-Cathode: stainless-steel capillary, 5 cm x 180 µm hole diameter, 1 mm from the surface
-Ar flow rate: 25 sccm
-Electrolyte: 1 mmol/L $AgNO_3$, target molecule=crystal violet (CV), de-ionized water
-V=290V and I=2mA
-time ranging=1-30 min

TEM images
(process time=10 min)
Mean particle diameter=7,5nm with standard deviation=2 nm

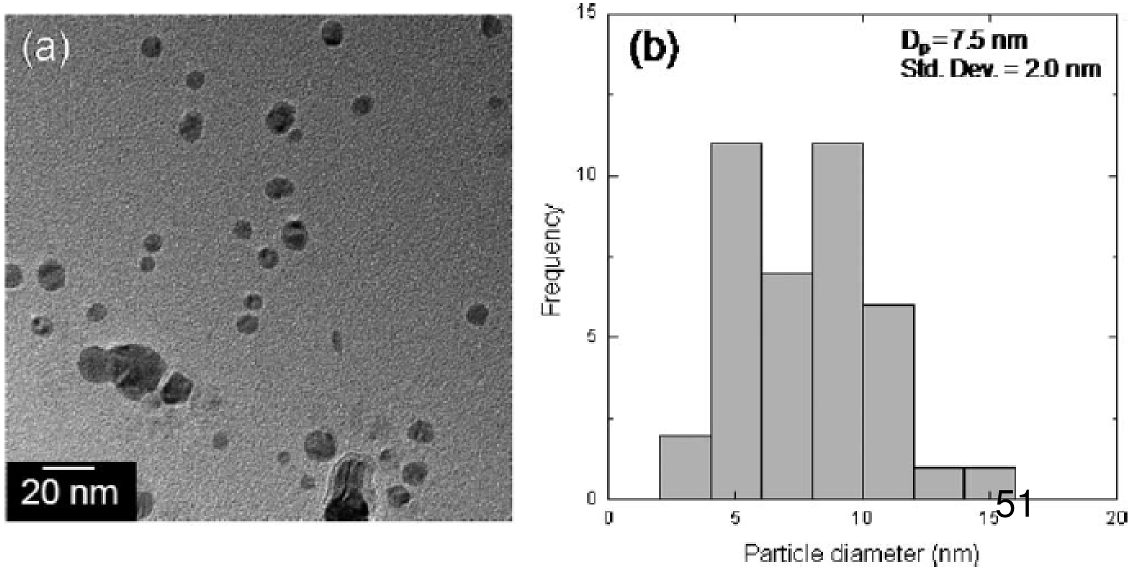

Microplasmas for environment

- Dissociation of CO_2
- Decomposition of Toluene

CO_2 dissociation by microplasmas

Taylan et al., PSST ***24*** *(2015) 015006, Austin, USA*

Patm; hole diameter=400µm
Electrodes=aluminium 10µm
Dielectric=mica 150 µm
Rballast=1 MΩ
DC voltage=2.5-4.5 kV
Flow rate=10-800 ml/min

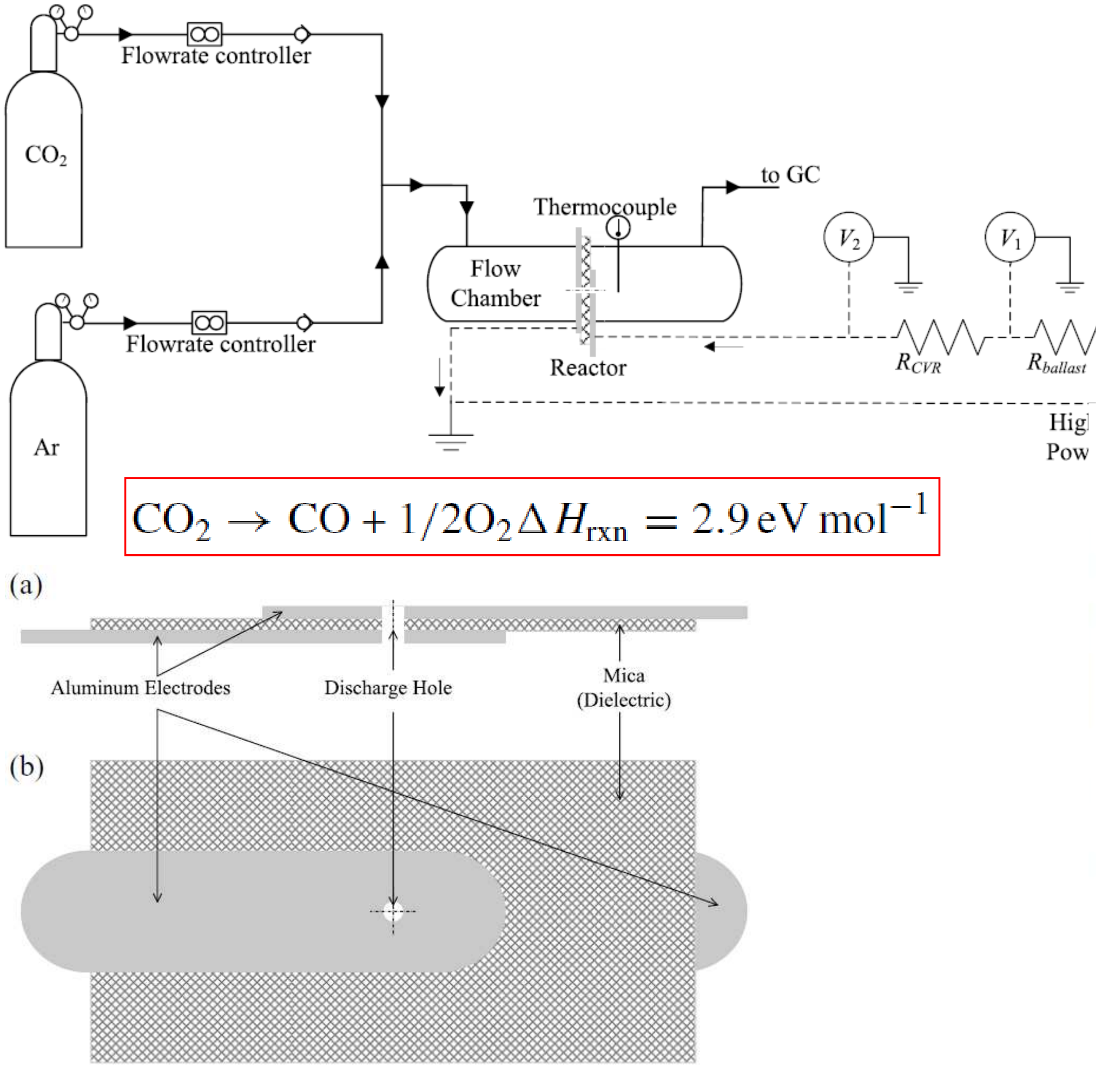

$$CO_2 \rightarrow CO + 1/2O_2 \Delta H_{rxn} = 2.9\,\mathrm{eV\,mol}^{-1}$$

Max yield=10.5%

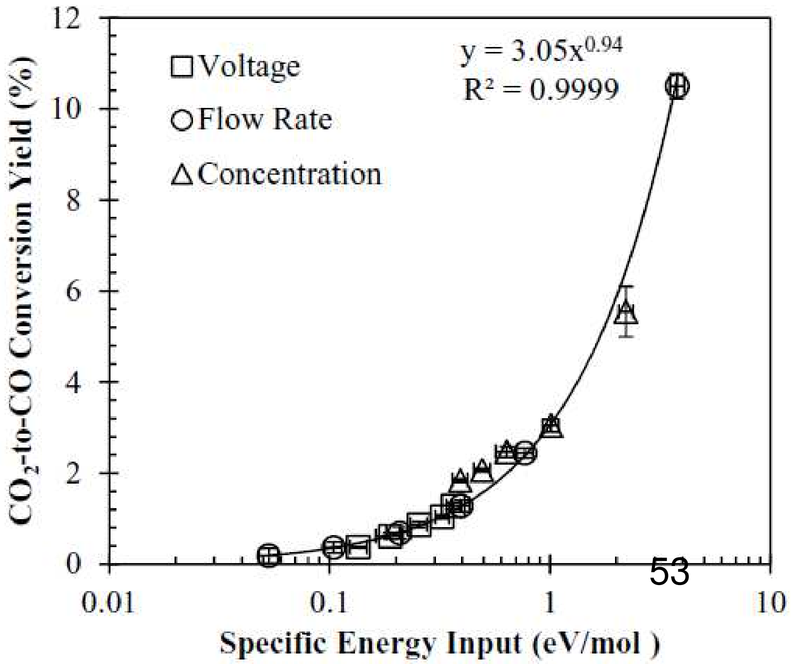

Decomposition of Toluene by microplasmas

Seto et al., J. J. Appl. Phys. ***44*** *(2005) 5206, Japan*

Surface discharge microplasma

Rectangular mica sheet:30 mm long, 20 mm wide, 80 µm thick

Electrodes: stainless steel, 100 µm wide, 80 µm thick

Measurement with GCMS and CO_2 analysis

66.7 kHz, 3.5 kV

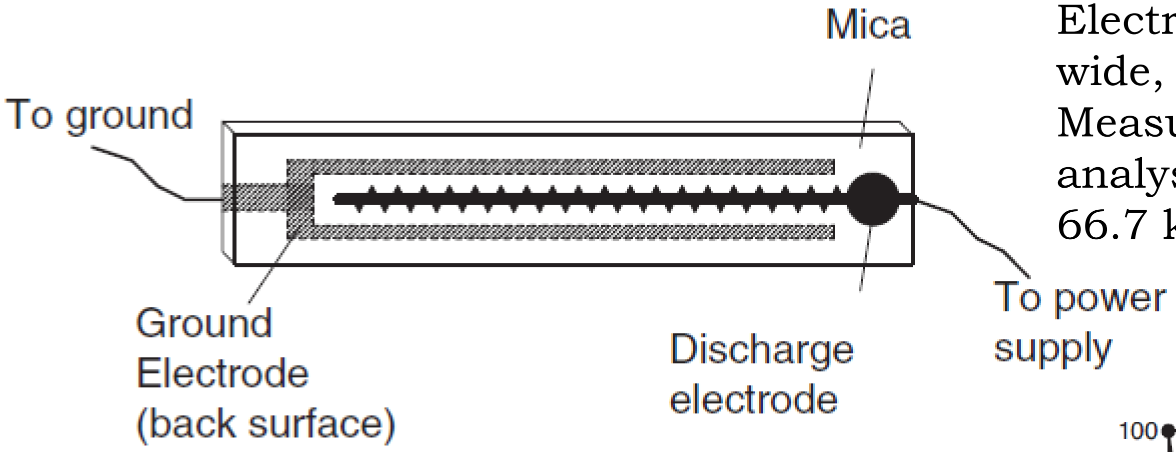

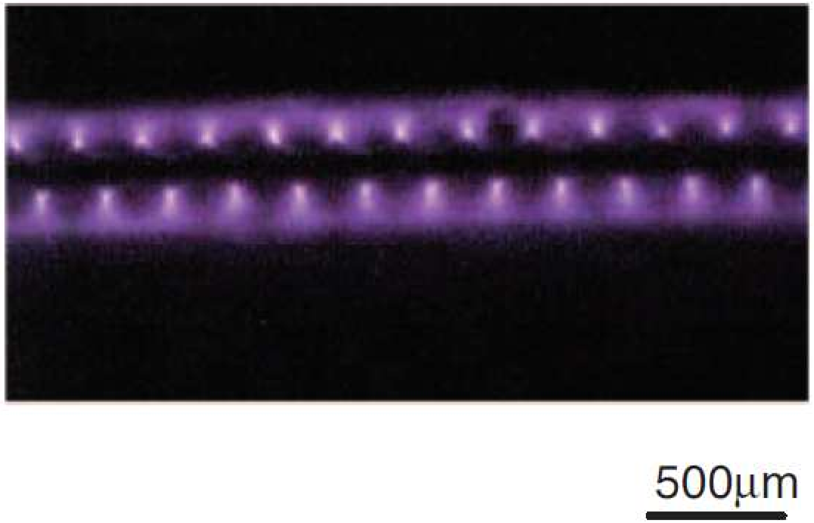

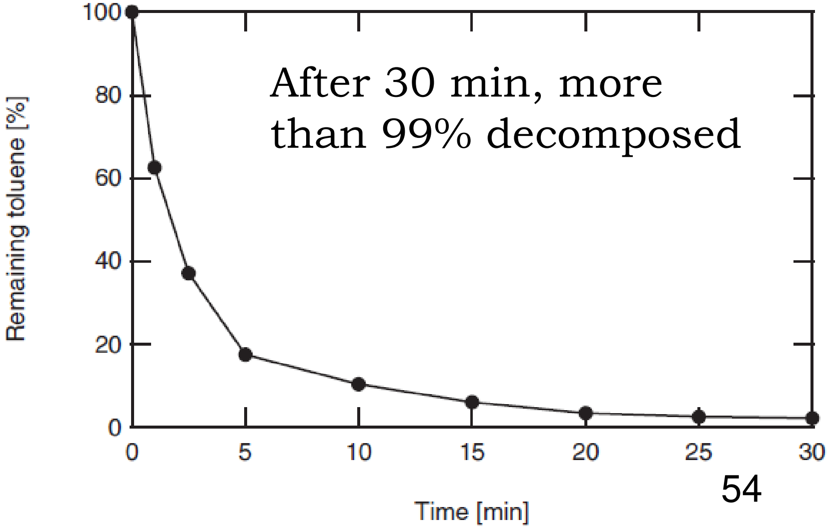

After 30 min, more than 99% decomposed

Microplasmas for medical applications

- Joao Santos Sousa’s presentation

Merci pour votre attention

LSPM-CNRS
Université Paris 13
99 Av J. B Clément
93430 Villetaneuse, France

www.lspm.cnrs.fr

Fax: +33 1 49 40 34 14

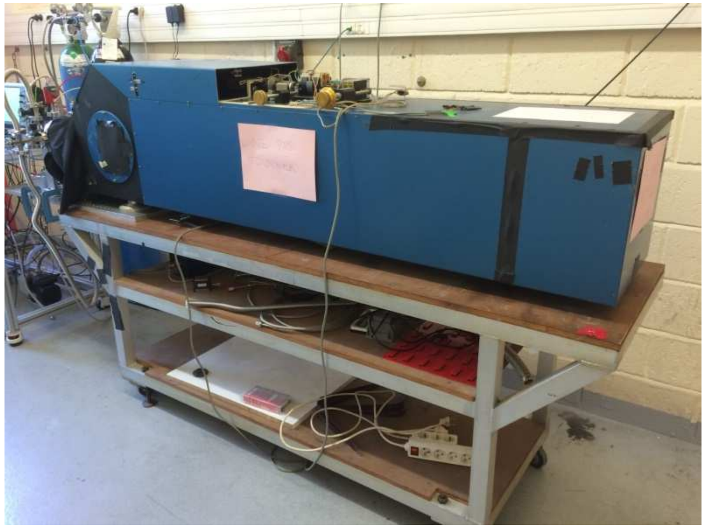

-f = 2 m

-1200 g/mm

-résolution spatiale = 2 µm

-dispersion spectrale: 0.788 pm/pixel

Spectromètre SOPRA haute-résolution (débitmètre H_2)
(outils réseau plasmas froids)